Unraveling the interplay between senescent dermal fibroblasts and cutaneous squamous cell carcinoma cell lines at different stages of tumorigenesis

Toutfaire, Marie; Dumortier, Elise; Fattaccioli, Antoine; Van Steenbrugge, Martine; Proby, Charlotte M.; Debacq-Chainiaux, Florence

Published in:
International Journal of Biochemistry and Cell Biology

DOI:
10.1016/j.biocel.2018.03.005

Publication date:
2018

Document Version
Peer reviewed version

Final version published in International Journal of Biochemistry and Cell Biology available at 10.1016/j.biocel.2018.03.005

Research article

Full title:

Unraveling the interplay between senescent dermal fibroblasts and cutaneous squamous cell carcinoma cell lines at different stages of tumorigenesis

Short title:

Interplay between senescent dermal fibroblasts and cSCC cell lines

Author list:

Marie Toutfaire[1], Elise Dumortier[1], Antoine Fattaccioli[1], Martine Van Steenbrugge[1], Charlotte M. Proby[2], Florence Debacq-Chainiaux[1*]

[1] URBC, NAmur Research Institute for LIfe Science (NARILIS), University of Namur, Namur, Belgium

[2] Department of Dermatology and Division of Cancer Research, Ninewells Hospital and Medical School, University of Dundee, Dundee, United Kingdom

* Corresponding author:

E-mail: florence.chainiaux@unamur.be; postal address: URBC, NAmur Research Institute for LIfe Science (NARILIS), University of Namur, Rue de Bruxelles, 61, 5000 Namur, Belgium

Word counts:

Title: 19 words

Abstract: 248

Introduction: 655

Methods: 1712

Results: 1876

Discussion: 1483

“Main text”: 5726

Research article

Full title:

Unraveling the interplay between senescent dermal fibroblasts and cutaneous squamous cell carcinoma cell lines at different stages of tumorigenesis

Short title:

Interplay between senescent dermal fibroblasts and cSCC cell lines

Author list:

Marie Toutfaire[1], Elise Dumortier[1], Antoine Fattaccioli[1], Martine Van Steenbrugge[1], Charlotte M. Proby[2], Florence Debacq-Chainiaux[1*]

[1] URBC, NAmur Research Institute for LIfe Science (NARILIS), University of Namur, Namur, Belgium

[2] Department of Dermatology and Division of Cancer Research, Ninewells Hospital and Medical School, University of Dundee, Dundee, United Kingdom

* Corresponding author:

E-mail: florence.chainiaux@unamur.be; postal address: URBC, NAmur Research Institute for LIfe Science (NARILIS), University of Namur, Rue de Bruxelles, 61, 5000 Namur, Belgium

Word counts:

Title: 19 words

Abstract: 248

Introduction: 655

Methods: 1712

Results: 1876

Discussion: 1483

“Main text”: 5726

Abstract

Cutaneous Squamous Cell Carcinoma (cSCC) is the second most common type of non-melanoma skin cancer in white-skinned populations. cSCC is associated with sun exposure and aging, which is concomitant with an accumulation of senescent cells in the skin. The involvement of senescent cells in carcinogenesis has been highlighted in several cancer types and an interaction between cSCC cells and senescent cells is proposed, but still little explored. Tumor-associated effects are mostly attributed to the senescence-associated secretory phenotype (SASP). Here, we compared two *in vitro* models of senescence, namely replicative senescence and UVB-stress induced premature senescence (UVB-SIPS), in human dermal fibroblasts and screened for expression of SASP-related genes in our models. Next, the impact of senescent fibroblasts on three cSCC isogenic cell lines, representing different stages of keratinocyte malignant transformation, was studied. Only a limited impact on cSCC cell lines' growth and migration has been detected with conditioned media collected from senescent fibroblasts and indirect co-cultures. We then investigated the opposite interaction and found that cSCC cell lines maintained in indirect co-cultures with fibroblasts induced and reinforced their senescence state as shown by an increased proportion of cells positive for the senescence-associated β-galactosidase activity and an increased expression of several SASP-related genes. Moreover, these effects were modulated according to the stage of tumorigenesis of the different cSCC cell lines used. Finally, cSCC cell lines-co-cultures are associated with NF-κB activation in HDFs. Understanding the interplay between tumor cells and their microenvironment may have important influences in cancer research and therapeutic strategies.

Keywords

- Senescence
- Skin
- Cutaneous squamous cell carcinoma
- Stress-induced premature senescence, SIPS
- UVB
- Senescence-associated secretory phenotype, SASP

Abbreviations

BME: Basal Medium Eagle; CCL2: C-C motif chemokine ligand 2; CM: conditioned medium; cSCC: cutaneous Squamous Cell Carcinoma; CTGF: connective tissue growth factor; CXCL1: C-X-C motif chemokine ligand 1; DMEM: Dulbecco's modified Eagle's medium; EGF: epidermal growth factor; EMT: epithelial-to-mesenchymal transition; FCS: Fetal Calf Serum; FGF2: fibroblast growth factor 2; GAPDH: glyceraldehyde-3-phosphate dehydrogenase; HDF: human diploid fibroblast; ICAM1: intercellular adhesion molecule 1; IGFBP3: insulin like growth factor binding protein 2; IκBα: nuclear factor-kappa B inhibitor alpha; IL: interleukin; MMP: matrix metallopeptidase; NF-κB: nuclear factor-kappa B; RS: replicative senescence; SA-βgal: senescence-associated β-galactosidase; SASP: senescence-associated secretory phenotype; SIPS: stress-induced premature senescence; TGFB1: transforming growth factor beta 1; TLDA: TaqMan Low-Density Array; TNF-α: tumor necrosis factor-alpha; UVR: ultraviolet radiation; Y: young.

1 Introduction

Non-melanoma skin cancers, including basal cell carcinoma (BCC) and cutaneous squamous cell carcinoma (cSCC), are the most common cancers in white-skinned populations (Leiter et al., 2014). Their rates of incidence are increasing steeply worldwide (Lomas et al., 2012). Therefore, identifying etiologic factors and understanding the underlying mechanisms represents an important challenge for health care services.

cSCC is associated with aging with an average age of 70 years old at diagnosis, and 80 % of cSCC occurring in people aged over 60 years old (Leiter et al., 2014). The main causal factor associated with development of cSCC is lifelong cumulative sunlight exposure. Skin aging is in large part 'photoaging' and is characterized by an accumulation of senescent cells in the skin (Dimri et al., 1995; Ressler et al., 2006; Toutfaire et al., 2017; Waaijer et al., 2012), raising the question of whether this accumulation of senescent cells and the appearance of cSCC with advancing age are in someway linked.

The involvement of senescent cells in carcinogenesis has been highlighted in several cancer types, such as breast and prostate cancers (Lasry and Ben-Neriah, 2015). They promote tumor cell growth, migration and invasion through induction of epithelial-to-mesenchymal transition (EMT) (Campisi, 2013; Naylor et al., 2013). These effects are mostly attributed to the senescence-associated secretory phenotype (SASP), which is composed of growth factors, cytokines, chemokines and proteases (Coppe et al., 2010; Freund et al., 2010). An impact of senescent cells has also been described in skin cancers. Senescent fibroblasts have been shown to enhance the early stages of skin carcinogenesis in post-senescence emergent keratinocytes through the involvement of the MMP/PAR-1 (matrix metallopeptidase/protease-activated receptor-1) axis (Malaquin et al., 2013). The

involvement of senescent fibroblasts is also described in melanoma initiation and metastasis via the secretion of soluble factors (Kaur et al., 2016; Kim et al., 2013). Senescent dermal fibroblasts also release chemerin, which promotes cSCC migration (Farsam et al., 2016). However, little is known about the crosstalk between senescent fibroblasts and cSCC cells, and particularly about a possible modulation according to their tumorigenesis stage.

Cellular senescence includes replicative senescence, associated with the critical telomere shortening, but also stress-induced premature senescence (SIPS) generated by DNA damage and/or oxidative stress and oncogene-induced senescence (OIS) following oncogene activation (Campisi, 2013; Debacq-Chainiaux et al., 2016). It is worth noting that even if these cells are irreversibly growth-arrested, some other senescence characteristics, such as the SASP, can be modulated according to the senescence inducer (Coppe et al., 2010). Therefore, senescence studies may inform on relevant senescence inducers within specific tissue contexts.

With reference to the skin, its aging is strongly influenced by environmental factors, notably solar radiation and particularly ultraviolet radiation (UVR) (Krutmann et al., 2017). Among them, UVB is the most energetic component of UVR to reach the earth's surface and UVB has been shown to induce a senescent phenotype in various skin cell types (Toutfaire et al., 2017).

In this study, we used two relevant *in vitro* models of senescence in the context of skin aging and cSCC, which are replicative senescence and UVB-induced senescence (UVB-SIPS, (Debacq-Chainiaux et al., 2005)) in dermal HDFs (human diploid fibroblasts). We investigated their SASP and their interaction with cSCC cell lines, using three isogenic cSCC cell lines that represent different stages of malignant transformation with the same genetic background (Proby et al., 2000). These stages of squamous epidermal carcinogenesis are carcinoma *in situ*, invasive

primary SCC and distant lymph node metastasis. Firstly, the interaction of senescent HDFs on cSCC cell lines was analyzed by using conditioned media and indirect co-cultures. Secondly, we studied the impact of these cSCC cell lines on HDFs by indirect co-cultures. Our results strongly suggest for the first time that cSCC cell lines highly induce and reinforce HDFs senescence, with an increase in senescence-associated β-galactosidase (SA-βgal) activity and in SASP-related genes expression. Interestingly these effects are modulated according to the tumorigenesis stage. Finally, cSCC cell lines-co-cultures are associated with NF-κB activation in HDFs.

2 Materials and methods

2.1 Cell culture

Dermal HDFs (AG04431 from Coriell Institute for Medical Research) were grown in BME (Basal Medium Eagle, Gibco) supplemented with 10 % FCS (Fetal Calf Serum, Gibco) and 2 mM L-glutamine (Gibco) until replicative senescence or submitted to UVB stresses to induce UVB-SIPS as previously described (Debacq-Chainiaux et al., 2005). For UVB-SIPS, HDFs were seeded at 8,000 cells per cm^2 and control cells were kept in the same culture conditions without UVB exposure.

PM1, MET1 and MET4 cell lines were isolated from the same individual and represent different stages of tumorigenesis (Proby et al., 2000). PM1 cell line is derived from dysplastic forehead skin and believed to represent carcinoma *in situ* or pre-invasive dysplasia; MET1 cell line is derived from a primary cSCC arising on dorsal hand and MET4 cell line is derived from an axillary lymph node metastasis from MET1. These keratinocytes cell lines were cultivated in DMEM plus Ham's F-12 Nutrient Mix (Gibco, ratio of 3:1) containing 10 % FCS, 400 ng/ml hydrocortisone (Sigma-Aldrich) and 10 ng/ml mouse EGF (AbD Serotec) as described previously

(Claerhout et al., 2010). A431 cSCC cell line was purchased from the American Type Cell Culture Collection (ATCC) and was grown in DMEM supplemented with 10 % FCS.

For positive control for NF-κB activation, HDFs were incubated with 20 ng/ml tumor necrosis factor-alpha (TNF-α, R&D Systems) for 30 min in BME with 1 % FCS and 2 mM L-glutamine. Negative control was kept in the same culture conditions without TNF-α incubation.

All cells were maintained at 37°C in a humidified atmosphere containing 5 % CO_2. Bright-field images of all the cell types used in this study are shown in Fig. S1.

2.2 Conditioned media and co-culture experiments

For conditioned media collection, HDFs were seeded at 5,300 (young) or 8,000 (replicative senescent) cells per cm^2 in BME with 1 % FCS and 2 mM L-glutamine. The next day, media were changed. For SIPS HDFs, media were changed 64 hours after the last UVB stress. Conditioned media were collected after 48 hours of incubation from HDFs with a similar density (approximately 55,000 cells/ml). The “BME” condition refers to medium incubated with glutamine and FCS but without fibroblast. After collection, media were centrifuged at 1,000 rpm for 7 min at 4°C to eliminate cell debris and they were used immediately without freezing.

For indirect co-culture experiments, the protocol is illustrated in Fig. 4. 10,000 dermal HDFs per cm^2 were seeded in 6-well plates (Corning) in BME with 1 % FCS and 2 mM L-glutamine. CTL-SIPS and UVB-SIPS HDFs were seeded at 72 hours after the last UVB stress. The next day (day 0), cSCC cell lines were seeded in cell culture inserts (membrane pore size of 0.4 μm, Corning). PM1, MET1 and MET4 were seeded at 2,100 cells/cm^2 in DMEM plus Ham’s F-12 Nutrient Mix containing 1

% FCS, hydrocortisone and mouse EGF. A431 were plated at 1,500 cells/cm^2 in DMEM with 1 % FCS. Media were changed at day 3 of co-culture.

2.3 TLDA analysis

Total RNA was isolated using the RNeasy Mini kit or Micro kit and Qiacube (Qiagen). RNA integrity and quality was validated with RNA 6000 Nano kit and 2100 Bioanalyzer (Agilent Technologies) and reverse-transcribed using the High-Capacity cDNA Reverse Transcription kit (Applied Biosystems). A customized TaqMan Low-Density Array (TLDA) allowing study of the expression of 48 SASP-related genes was generated (list of the genes on Table S1). TLDA analyses were performed using TaqMan™ Universal PCR Master Mix no AmpErase UNG and ViiA7 instrument according to the manufacturer's instructions (Applied Biosystems). Relative abundance was determined with the $\Delta\Delta$Cq method, normalized to the mRNA abundance of *GAPDH* (glyceraldehyde-3-phosphate dehydrogenase) for Table 1 and *GAPDH* and *RNA18S* for Table 2 and expressed as relative to the stated control.

2.4 Cell growth measurement

For conditioned media experiments, 16,000 cells/cm^2 for PM1 and 8,000 cells/cm^2 for MET1, MET4 and A431 cell lines were seeded in 12-well plates in their respective medium with 1 % FCS and incubated the next day with conditioned media for 24 hours. For co-culture experiments, cell culture insert membranes were cut off carefully with a blade and put in 6-well plates at day 1, 3 and 6 of co-culture.

Cell growth was measured with the CellTiter 96 AQueous One Solution Cell Proliferation Assay (Promega). Cells were incubated 3 hours with 200 µl of reagent in 1 ml of culture medium at 37°C in a humidified, 5 % CO_2 atmosphere. The absorbance was then measured at 490 nm. To avoid background, we calculated

corrected absorbance by subtracting the absorbance of control wells (containing medium and reagent without cells).

2.5 Migration and invasion assays

For migration assays, 30,000 cells/well for PM1, 10,000 cells/well for MET1 and 15,000 cells/well for MET4 and A431 cell lines were seeded onto Falcon cell culture inserts with 8 μm pore size (24-well plates, Corning) in their respective medium with 1 % FCS. For invasion assays, MET1 (10,000 cells/well), MET4 (15,000 cells/well) and A431 (30,000 cells/well) cell lines were seeded onto BioCoat Matrigel Invasion Chambers with 8 μm pore size coated with Matrigel Matrix (24-well plates, Corning) in their respective medium with 1 % FCS following manufacturer's instructions. Conditioned media were incubated in the lower chambers for 24 hours at 37°C in a humidified, 5 % CO_2 atmosphere. Cells on the lower surface of the membrane were rinsed, fixed and stained with 0.2 % crystal violet in 2 % aqueous ethanol (Merck Millipore) for 2 min. After several washes in distilled water, the non-migrating and non-invading cells were removed from the upper surface by twice scrapings with cotton swabs (Copan). Membranes were photographed with the BX-63 microscope (Olympus, magnification 4 x) and analyzed for cell counting.

2.6 Senescence-associated beta-galactosidase (SA-βgal) activity

At day 1 and 6 of co-culture, HDFs were seeded in 6-well plates (Corning) at a density of 1,000 cells/cm^2 in DMEM plus Ham's F-12 Nutrient Mix containing 1 % FCS, hydrocortisone and mouse EGF. The next day SA-βgal staining was performed as described in (Dimri et al., 1995) during 16 hours. The proportion of SA-βgal positive cells was determined by counting 400 cells per well.

2.7 RT-qPCR analysis

Total RNA was isolated using the RNeasy Micro kit and Qiacube (Qiagen) and reverse-transcribed using Transcriptor First Strand cDNA Synthesis Kit (Roche) following manufacturer's instructions. qPCR was performed using SYBR Green PCR Master mix (Roche), primers and the StepOnePlus Real-Time PCR system (Applied Biosystems). Primers used were: CCL2-F: CATTGTGGCCAAGGAGATCTG; CCL2-R: AGTGAGTGTTCAAGTCTTCGGAGTT; GAPDH-F: ACCCACTCCTCCACCTTTGAC; GAPDH-R: GTCCACCACCCTGTTGCTGTA; IL1B-F: GCCCTAAACAGATGAAGTGCTC; IL1B-R: GAGATTCGTAGCTGGATGCC; IL8-F: CTGGCCGTGGCTCTCTTG and IL8-R: GGGTGGAAAGGTTTGGAGTATG. Relative abundance was determined with the ΔΔCq method, normalized to the mRNA abundance of *GAPDH* and expressed relative to the stated control.

2.8 Nuclear p65 staining

HDFs were analyzed at day 6 (or day 3) of co-culture directly in 6-well plates. Cells were fixed with 4 % paraformaldehyde in PBS (Merck Millipore) for 10 min, permeabilized in 1 % Triton X-100 (Sigma-Aldrich) in PBS for 5 min and incubated with rabbit anti-NF-κB p65 antibody (1:400, Cell Signaling, AB_10859369) diluted in 3 % bovine serum albumin (Santa Cruz Biotechnology) in PBS overnight at 4°C. Cells were then incubated with the secondary antibody Alexa Fluor 488 goat anti-rabbit IgG (1:1,000, Molecular Probes, AB_143165) diluted in 3 % bovine serum albumin in PBS for 1 hour at room temperature. Nuclei were stained with DAPI (1ng/ml in PBS, Sigma-Aldrich) during 15 minutes at room temperature. Cells were kept in PBS in the dark and analyzed with the BD Pathway 855 (BD Biosciences). Segmentation and analyses were performed with BD AttoVision software, which identified nuclei through DAPI staining and quantified the NF-κB p65 staining

intensity in these regions of interest. An average of 450 cells was counted per condition.

2.9 Western blot analysis

Total cell protein lysates were obtained using a buffer containing 40 mM Tris (Merck Millipore), 150 mM KCl (Merck Millipore), 1 mM EDTA (Merck Millipore), pH 7.5, 1 % Triton X-100 (Sigma-Aldrich), supplemented with Complete Protease Inhibitor Cocktail (Roche) and 4 % phosphatase inhibitor buffer (25 mM Na_3VO_4 (Sigma-Aldrich), 250 mM 4-nitrophenyl phosphate (Sigma-Aldrich), 250 mM β-glycerophosphate (VWR), 125 mM NaF (Merck Millipore)). Protein concentration was determined by Pierce 660 nm Protein Assay (Thermo Scientific). 8 μg of proteins were separated by SDS-PAGE on 10 % SDS-PAGE gels and electrotransferred on a polyvinylidene fluoride membrane (Merck Millipore). Molecular weights were determined with color pre-stained protein standard (New England Biolabs). Membranes were blocked 1 hour at room temperature in Odyssey blocking buffer (LI-COR) and then overnight at 4°C in Odyssey blocking buffer with 0.1 % Tween 20 (Bio-Rad) containing a primary antibody. The primary antibodies used are rabbit anti-IκBα (1:500, Santa Cruz Biotechnology, AB_2235952) and mouse anti-β-actin (1:10,000, Sigma-Aldrich, AB_476744). After 4 washes of 5 minutes in PBS with 0.1 % Tween 20, the incubation with the secondary antibody (IRDye 680RD goat anti-rabbit IgG, LI-COR, AB_621841 or IRDye 680RD goat anti-mouse IgG, LI-COR, AB_10956588, both 1:10,000) was performed for 1 hour in Odyssey blocking buffer with 0.1 % Tween 20. After 4 washes of 5 minutes in PBS-Tween and 2 washes in PBS, the membrane was dried 1 hour at 37°C and scanned using Image Studio Lite software V3.1.4 (LI-COR) for the quantification.

2.10 Statistical analysis

Experiments were performed at least three times independently except when otherwise noted. Results are expressed as means ± SEM (standard error of the mean). Statistical analyses were performed using R software (version 3.2.3 from the R Foundation for Statistical Computing).

Two-tailed T-test (Table 1, Fig. 9A, 10C and Fig. S7A) or two ways analysis of variance with *post-hoc* Tukey's test were performed. For Fig. 1-3, 5, 10 and Fig. S6, S12, each experiment was treated as a matched set to anticipate experiment-to-experiment variability and was considered as one factor of the ANOVA. Normality and homoscedasticity of the data were assessed with Shapiro-Wilk and Levene's test respectively. When normality or homogeneity of variances could not be assumed (p-value < 0.05), statistical analyses were performed on transformed data (log-transformed data for Tables 1-2, Fig. 1B-C, 3, 5, 7, 8, and Fig. S6 or square-root-transformed data for Fig 6). In order to facilitate interpretation, untransformed data are shown. When normality or homoscedasticity tests failed on transformed data (p-value < 0.05), Kruskal-Wallis test followed by Wilcoxon-Mann-Whitney test were performed instead (Fig. 7A, 8A and 8C).

3 Results

3.1 Dermal HDFs in replicative or in UVB-induced senescence display specific SASP-related gene expression changes

To determine the expression of SASP-related genes in HDFs in replicative senescence (RS) or in UVB-SIPS, we designed a customized TLDA (Applied Biosystems) to analyze simultaneously the expression of 48 SASP-related genes (Table S1). HDFs in RS displayed a significant increase in *IL1B* (interleukin 1 beta),

ICAM1 (intercellular adhesion molecule 1), *CTGF* (connective tissue growth factor) and *IL6* relative mRNA abundances when compared with pre-senescent (young) HDFs (Table 1A). They also displayed a significant decrease in several SASP-related gene abundances, such as *CXCL1* (C-X-C motif chemokine ligand 1) and *CXCL2*. HDFs in UVB-SIPS shared three common expression changes with RS, the increased *IL1B*, *IL6* and *CTGF* relative mRNA abundances (Table 1B). UVB-SIPS HDFs also displayed a significant increase in *MMP1, MMP3*, *CXCL1, CXCL2, CCL2* (C-C motif chemokine ligand 2)*, IL8, IGFBP3* (insulin like growth factor binding protein 2)*, IGFBP6*, *FGF2* (fibroblast growth factor 2) *and TGFB1* (transforming growth factor beta 1) relative mRNA abundances when compared with their respective control (CTL-SIPS), not exposed to UVB exposure. These results highlighted that HDFs in RS or in UVB-SIPS are characterized by common but also by specific expression changes for SASP-related genes, which may be reminiscent of differential impacts on their microenvironment.

3.2 Limited impact of senescent dermal HDFs on cSCC cell lines growth, migration and invasion according to their stage of tumorigenesis

The impact of dermal senescent HDFs on cSCC is poorly described. The aim of our present study was first to see if this impact could be modulated *in vitro* according to the stage of tumorigenesis of this type of cancer. For this purpose, cSCC lines isolated from the same individual and representing different stages of tumorigenesis (Proby et al., 2000) were selected. PM1 cell line is derived from dysplastic skin and represents early stage of malignant transformation; MET1 cell line is derived from a primary SCC with invasive properties and MET4 cell line is derived from a distant metastasis (Proby et al., 2000). These cell lines represent

therefore an isogenic skin cancer progression model (Barrette et al., 2014). We validated that they displayed different expression patterns of EMT markers as described previously (Fig. S2). All cSCC cell lines were subsequently used at low passage numbers, with marked differences for EMT markers.

We first tested the impact of conditioned medium collected after 48 hours of culture from senescent HDFs in RS or in UVB-SIPS and their respective controls (young and CTL-SIPS; see Fig. S3 for bright-field images of HDFs) on the growth, the migration and the invasion of the cSCC cell lines after 24 hours of incubation. No significant impact of conditioned medium from HDFs in RS or in UVB-SIPS was observed, except for a growth increase for PM1 incubated with UVB-SIPS conditioned medium (Fig. 1-3; see Fig. S4 and S5 for bright-field images of migrating and invading cells). Moreover, a negative and not negligible impact of these conditioned media was noticed compared to the medium alone.

Since the impact of senescent HDFs on cSCC cell migration (including the A431 cell line) has been shown recently (Farsam et al., 2016), the impact of our conditioned media on A431 cells was analyzed (Fig. S6). As expected, replicative senescent HDFs conditioned media promoted A431 cell line migration when compared with young HDFs conditioned media (Fig. S6B). However, they did not affect A431 cell line growth or invasion (Fig. S6A and S6C). Moreover, UVB-SIPS HDFs conditioned media did not show any effect.

Indirect co-culture experiments were then performed by using cell culture inserts. Indirect co-cultures have several advantages among which the population-specific detection of cellular changes and the bidirectional exchange. Senescent HDFs (in RS or in UVB-SIPS), or not (young or CTL-SIPS), were seeded in the dish and cultivated with cSCC cell lines at different stages of tumorigenesis in the above inserts (Fig. 4). We first studied the impact of HDFs' senescence on cancer cell

growth. To assess our co-culture protocol, the impact of young or replicative senescent WI-38 co-cultures on MDA-MB-231 growth, which has been described previously (Krtolica et al., 2001), was evaluated. As expected, replicative senescent WI-38 significantly promoted MDA-MB-231 growth from 5 days of co-culture when compared with young WI-38 (Fig. S7).

Co-cultures were then performed with HDFs in RS or in UVB-SIPS, or with their respective controls (young or CTL-SIPS), and cSCC cell lines at different stages of tumorigenesis. We did not detect any difference in growth for PM1, MET1 and MET4 maintained in co-cultures with senescent HDFs, except for PM1 maintained with UVB-SIPS HDFs (at day 1) and for MET4 maintained with RS HDFs (at day 1 and at day 6) (Fig. 5; see Fig. S8 for bright-field images of cSCC cell lines during co-cultures). These results confirm the ones obtained with the conditioned media and, despite being reproducible and significant, it would seem that the impact of the senescent HDFs on these three cSCC cell lines is rather limited. This result is surprising but shows that the pro-tumorigenic effect of senescent HDFs is not universal, and that it may depend on the senescence model and on the type of cancer cell.

3.3 cSCC cell lines influence dermal HDFs senescence

Next, we chose to investigate the two-way exchange by studying the impact of cSCC cells on HDFs. Whilst the impact of senescent cells on their microenvironment is highly described, little is known about the opposite interaction. We focused this investigation on replicative senescence. Thus, the impact of cSCC cell lines on the SA-βgal activity of young and RS HDFs, at day 1 and day 6 of the co-cultures, was measured (Fig. 6; see Fig. S9 for bright-field images of SA-βgal activity detection in HDFs). Interestingly, after 6 days of co-culture, a higher proportion of SA-βgal

positive cells was detected in young HDFs co-cultured with PM1, MET1 and MET4, when compared with the control condition (young HDFs alone). This effect was more pronounced in MET1- and MET4-co-cultures, when compared to PM1-co-culture. No co-culture effect was observed in replicative senescent HDFs.

3.4 cSCC cell lines highly increase SASP-related gene expression in dermal HDFs

We then investigated the impact of PM1 and MET1-co-cultures on SASP-related gene expression in HDFs (Table 2) using the same customized TLDA (Table S1). RNA was isolated after 1 or 6 days of co-culture in young and replicative senescent HDFs. This screening showed that senescence (between young and RS HDFs) and/or co-culture (between HDFs alone or co-cultured with PM1 or MET1) modulated several SASP-related gene expression changes after 6 days of co-culture.

For young and replicative senescent HDFs, the relative expression level of four genes (*CCL2, CXCL2, IL1B* and *MMP1*) was significantly increased with senescence and co-culture (Table 2). Indeed, PM1 and MET1 cell lines-co-cultures induced a significant gene expression increase in young and replicative senescent HDFs, when compared with their respective controls (alone). Only the expression of *TIMP2* (*TIMP metallopeptidase inhibitor 2*) was significantly increased with senescence, but reduced with co-culture (with PM1 cell line). Moreover, an induction of the mRNA abundance of four other genes (*CCL20*, *CXCL1*, *ICAM1* and *IL8*) was also observed with co-culture. Finally, *FGF2*, *IGFBP3*, *IGFBP5*, *MMP3*, *MMP10* and *TNFRSF11B* gene expression were upregulated, and *IGFBP2*, *PTGS1* (*prostaglandin-endoperoxide synthase 1*) and *VCAM1* (*vascular cell adhesion molecule 1*) gene expression were downregulated with senescence.

To confirm these results on a larger sample size, we studied *CCL2*, *IL1B* and *IL8* gene expression in co-cultures of young and replicative senescent HDFs with PM1, MET1 and MET4 cells (Fig. 7; see Fig. S10 for bright-field images of HDFs during co-cultures). The three genes were overexpressed in RS HDFs at day 1 of the co-culture. After 6 days of co-cultures, a significant increase of these three genes in young and in RS HDFs when co-cultured with the three cSCC cell lines was observed. Moreover, for *IL1B* and *IL8* gene expression, the co-culture impact was higher with MET1-co-culture, when compared with MET4-co-culture, showing a similar effect but with an amplitude dependent on the tumorigenesis stage.

Thus, co-cultures seem to induce and to reinforce the senescent state of HDFs.

In order to confirm these results with another cSCC cell line isolated from another patient, we performed co-culture experiments with A431 cell line (Fig. 8; see Fig. S11 for bright-field images of HDFs during co-cultures). As this cell line was highly proliferative, co-culture experiments were stopped at day 3, when cell confluence was reached. We confirmed the overexpression of these three genes in RS HDFs at day 1, and in young and RS HDFs maintained in co-culture with A431 cells at day 3.

3.5 cSCC cell lines-co-cultures are associated with NF-κB activation in dermal HDFs

As the cSCC cell lines induced an increase in SASP-related gene expressions in HDFs, we can wonder if regulatory networks of the SASP are activated. NF-κB (nuclear factor-kappa B) is one master regulator of most SASP-related gene expressions (Malaquin et al., 2016). As p65 is an essential subunit of the NF-κB complex, we investigated the nuclear p65 staining intensity in HDFs alone or co-

cultured with cSCC cell lines in order to highlight a possible activation (Fig. 9). TNF-α treated HDFs provided a positive control for p65 nuclear activation (Fig. 9A).

The fluorescence intensity of nuclear p65 per cell was significantly increased in RS HDFs when compared with young HDFs (Fig. 9B and 9C), as expected (Malaquin et al., 2016). Moreover after 6 days of co-culture, there was a significant impact of PM1 and MET4-co-cultures on young and RS HDFs' staining when compared with the control conditions alone. This is consistent with our previous results that showed that cSCC cell lines-co-cultures promoted SASP-related gene expressions. Surprisingly there was no significant impact of MET1-co-cultures when compared with the control conditions alone on nuclear p65 intensity staining. Finally, this staining intensity was also increased in young HDFs co-cultured with A431 cells for 3 days when compared with young HDFs alone (Fig. 9C).

In order to confirm the possible activation of NF-κB in HDFs during co-cultures, we performed western blot analyses of IκBα (NF-κB inhibitor alpha), which is one of the inhibitory proteins of NF-κB (Fig.10 and Fig. S12). In unstimulated cells, IκB interacts with NF-κB dimers in the cytoplasm, therefore preventing their nuclear translocation (Capece et al., 2017). However, upon NF-κB activation, IκB kinases (IKKs) trigger the phosphorylation and the proteasomal degradation of IκB (in particular IκBα), which allows NF-κB dimers to translocate to the nucleus and to activate target genes' transcription. As expected, we showed that IκBα protein abundance in total protein extracts from TNF-α treated HDFs was significantly reduced, which provided a positive control for NF-κB activation (Fig. 10A and 10C).

Interestingly, we also detected a significant decrease of the relative abundance of IκBα in young and RS HDFs co-cultured with PM1, MET1 and MET4 cell lines, when compared with the control conditions alone after 6 days of co-culture (Fig. 10B and 10D). This suggests that IκBα is degraded, allowing activation and

nuclear translocation of NF-κB. No significant impact of A431 cell line on IκBα protein abundance in HDFs was detected (Fig. S12).

Altogether, these results are consistent with p65 nuclear translocation and the induction of SASP-related gene expressions in HDFs, which strongly suggests that NF-κB is activated in HDFs during co-cultures with cSCC cell lines.

4 Discussion

It is well known that senescent cells enhance growth, migration and invasion of cancer cells, notably through their SASP (Campisi, 2013; Lasry and Ben-Neriah, 2015; Naylor et al., 2013). However, little is known about their impact on cSCC carcinogenesis, which is linked with aging and cumulative sun exposure (Leiter et al., 2014).

In senescence studies, attention should be paid to the use of relevant cellular senescence models, namely cell type and senescence inducer, which must be ideally selected according to the tissue context. Indeed, some senescence biomarkers, such as the SASP, might be highly modulated (Coppe et al., 2010; Toutfaire et al., 2017). As established that both chronological aging and UVR-induced photoaging, notably UVB, affect skin aging and cSCC development (Krutmann et al., 2017; Leiter et al., 2014), two relevant models of fibroblast senescence were compared, namely RS and UVB-SIPS HDFs. We showed in this study that both models display a significant increase in some SASP-related gene expressions. Interestingly, all these genes have been previously mentioned in SASP studies, such as those performed in other strains of senescent dermal HDFs (Freund et al., 2010; Lasry and Ben-Neriah, 2015).

It is well documented that RS and SIPS share common senescence biomarkers (Toussaint et al., 2002). We highlighted here that RS and UVB-SIPS

HDFs display some common SASP-related gene expression changes, notably an increase in *IL1B* and *IL6* mRNA expression. In this regard, mass spectrometric analyses and cytokine multiplex assay have shown that IL-1β is overexpressed in supernatant from intrinsically aged dermal HDFs (Waldera Lupa et al., 2015). Moreover, a previous study has also described that *IL1B* mRNA level is increased in UVB-SIPS HDFs (Debacq-Chainiaux et al., 2005). For *IL6*, its mRNA level is increased in RS dermal HDFs compared to young ones (Malaquin et al., 2013). Immunofluorescence staining has also showed that IL-6 expression in senescent stromal cells is significantly increased in skin from old individuals compared to younger individuals (Ruhland et al., 2016). Finally, *IL6* mRNA and protein level are significantly increased in dermal HDFs after UVB irradiation compared to non-irradiated HDFs (Brenneisen et al., 1999).

Interestingly, we also demonstrated specific gene expression changes between our two models of senescence. Indeed, a significant decrease in *CXCL1* and *CXCL2* gene expression in RS HDFs was highlighted. These decreases are also described in senescent HDFs from chronic wounds using Affymetrix microarray analysis and ELISA quantitation of conditioned medium (Wall et al., 2008). For UVB-SIPS HDFs, we showed an increase in *MMP1* and *MMP3* mRNA level. In this regard, it is known that dermis of photo-aged skin display higher levels of MMP1 protein level compared to sun-protected skin from the same individuals (Chung et al., 2001). Moreover, supernatant from UVB-irradiated dermal HDFs also display an increase in MMP1 and MMP3 protein level compared to non-irradiated HDFs (Brenneisen et al., 1999). Finally, an increase in *CTGF*, *IGFBP3* and *TGFB1* mRNA level and both latent and active forms of TGFB1 was also described in UVB-SIPS HDFs (Debacq-Chainiaux et al., 2005).

The specific SASP-associated gene expression signature observed in our

study between RS and UVB-SIPS HDFs is somewhat reminiscent of the “molecular scars” observed between RS and subcytotoxic stresses (Aan et al., 2013; Debacq-Chainiaux et al., 2008; Dierick et al., 2002a; Dierick et al., 2002b). This reinforces the need to use complementary models of senescence according to the tissue context.

It is worth noting that the secretome of senescent HDFs has been previously involved in skin carcinogenesis. For instance, MMPs secreted by senescent dermal HDFs promote migration of post-senescence emergent keratinocytes, an early event in skin cancer development (Malaquin et al., 2013). Moreover, secreted frizzled-related protein 2 (sFRP2) in the secretome of HDFs from aged donors induce melanoma cell invasion (Kaur et al., 2016). In our study, we analyzed the impact of RS and UVB-SIPS HDFs conditioned media on growth, migration and invasion of cSCC cell lines but only a limited impact was observed. These negative results might reflect the cSCC model, since we used skin-derived HDFs and cSCC cell lines. In a previous study, however, stimulation of keratinocytes with senescent HDFs conditioned media was achieved from the beginning of the culture until post-senescence emergence, which corresponds to about 45 days of stimulation (Malaquin et al., 2013). This long-term exposure, compared to short-term exposure, supports a pro-EMT effect of senescent fibroblasts’ secretome on keratinocytes. This might partly explain why we observed limited effects since cSCC cell lines were only exposed for 24 hours with conditioned media, even if short-term exposure remains the usual protocol (Farsam et al., 2016; Kaur et al., 2016; Kim et al., 2013).

Next the impact of senescent HDFs during indirect co-cultures was analyzed. This allows bidirectional exchanges with cSCC cell lines. Again, a very limited impact of senescent HDFs on cSCC growth was detected.

Finally, we analyzed the impact of cancer cell lines on HDFs, which is poorly investigated in senescence studies. Our results highlighted that cSCC cell lines in

indirect co-cultures reinforce HDFs' senescent traits. Indeed, after co-culture with all cSCC cell lines, an increase in the proportion of SA-βgal positive cells was detected in young, but not in RS, HDFs when compared with the control condition. Next, SASP expression at the mRNA level was studied. Interestingly, our screening showed that co-cultures with PM1 and MET1 mostly induced a significant gene expression increase in young and RS HDFs, when compared with their respective controls (alone). These results were confirmed for *CCL2*, *IL1B* and *IL8* mRNA expressions on a larger sample size and with A431, another cSCC cell line. These over-expressions are particularly interesting given that these cytokines are widely known to be involved in carcinogenesis. Indeed, CCL2, also known as monocyte chemoattractant protein-1, has a key role in the infiltration of inflammatory cells and in tumor immunity (Kalluri, 2016). Moreover, CCL2 secreted by $FSP1^+$ (fibroblast specific protein-1) fibroblasts may maintain local inflammation, which promotes skin carcinogenesis in DMBA/TPA- (7,12 Dimethylbenzanthracene/12-O-Tetradecanoyl Phorbol 13-Acetate) induced skin cancer in mouse (Zhang et al., 2011). Regarding IL-1β, which is a secreted form of IL-1, an involvement in inflammatory response (Kalluri and Zeisberg, 2006) and in tumor invasiveness is described (Dinarello, 1996). Finally, IL-8 has pro-angiogenic activities and is also involved in tumor progression and immunity (Coppe et al., 2010; Kalluri, 2016).

These increases in pro-inflammatory gene expression after co-culture with cancer cells are consistent with a previous study, which highlighted an education of dermal fibroblasts by carcinoma cells in K14/HPV16 mouse (Erez et al., 2010). These data have showed that dermal fibroblasts display an induction of their inflammatory gene signature after incubation with conditioned media from a skin carcinoma cell line *ex vivo* and *in vivo*.

The over-expression of SASP-related genes was more pronounced in co-culture with MET1, the highly invasive primary cSCC cell line. Similarly, CCL2, IL-1β and IL-8 are also up-regulated at the mRNA and protein levels in dermal HDFs co-cultured or exposed to conditioned media from several invasive melanoma cell lines when compared to a non-invasive one (Li et al., 2009). In this respect, this entails an increase in the invasive potential of melanoma cell lines upon co-culture with HDFs compared to stimulation with fibroblast-conditioned media. These bidirectional interactions are also described between cancer-associated fibroblasts and tumor cells, which involved chemokines (Mishra et al., 2011), and may appear similar to the crosstalk observed in our study.

The mechanisms inducing SASP-related over-expression during co-culture were then investigated. Our results strongly suggest that NF-κB, a master regulator of the mRNA expression of most SASP factors (Malaquin et al., 2016), is activated in HDFs during co-cultures. Indeed, we detected a significant increase in nuclear p65 staining in young and RS HDFs co-cultured with PM1 and MET4. Interestingly, an increase in nuclear p65 staining in stromal fibroblasts is also observed in skin section from K14/HPV16 mouse but not in control mice skin (Erez et al., 2010). A significant decrease of IκBα, which is reminiscent of NF-κB activation (Capece et al., 2017), was also observed in protein extracts from young and RS HDFs co-cultured with PM1, MET1 and MET4. However, other mechanisms might also be involved in SASP expression, such as the increased activity of C/EBPβ (CCAAT/enhancer binding protein beta), the other major transcription factor involved in senescence secretome (Freund et al., 2010; Malaquin et al., 2016). The possible signaling between cSCC cell lines and HDFs is presented in Fig. 11.

In summary, our results demonstrate cellular interactions within the cSCC microenvironment and support the use of co-culture experiments in addition to

conditioned media approaches. These data strongly suggest that signaling from cSCC cell lines induce senescence and SASP expression in young HDFs and reinforce SASP expression in RS HDFs. The question that remains open is whether these results might explain the accumulation of senescent cells at site of malignant transformation (He and Sharpless, 2017; Naylor et al., 2013). Overall, understanding the interplay between tumor cells and their microenvironment may have important outcomes in cancer research and therapeutic strategies.

Acknowledgments

Marie Toutfaire and Florence Debacq-Chainiaux are respectively recipient of a Télévie grant and research associate at FRS-FNRS (National Funds for Scientific Research, Belgium). The authors thank Maude Fransolet (URBC, University of Namur, Belgium) and the MORPH-IM (Morphology & Imaging) platform (University of Namur, Belgium) for their technical support with the BD Pathway 855 equipment; and the SAGE (Stress and AGEing) group (URBC, University of Namur, Belgium) for their technical help.

Conflicts of interest

The authors declare no conflict of interest.

Author Contributions

M.T. designed, performed and analyzed the experiments and wrote the manuscript; E.D., A.F. and M.VS. performed some experiments; C.M.P. provided the PM1, MET1 and MET4 cell lines and revised the manuscript; F.D-C supervised the work and revised the manuscript.

Reference list

Aan, G.J., Hairi, H.A., Makpol, S., Rahman, M.A., Karsani, S.A., 2013. Differences in protein changes between stress-induced premature senescence and replicative senescence states. Electrophoresis 34(15), 2209-2217.

Barrette, K., Van Kelst, S., Wouters, J., Marasigan, V., Fieuws, S., Agostinis, P., van den Oord, J., Garmyn, M., 2014. Epithelial-mesenchymal transition during invasion of cutaneous squamous cell carcinoma is paralleled by AKT activation. Br J Dermatol 171(5), 1014-1021.

Brenneisen, P., Wlaschek, M., Wenk, J., Blaudschun, R., Hinrichs, R., Dissemond, J., Krieg, T., Scharffetter-Kochanek, K., 1999. Ultraviolet-B induction of interstitial collagenase and stromelyin-1 occurs in human dermal fibroblasts via an autocrine interleukin-6-dependent loop. FEBS Lett 449(1), 36-40.

Campisi, J., 2013. Aging, cellular senescence, and cancer. Annu Rev Physiol 75, 685-705.

Capece, D., Verzella, D., Tessitore, A., Alesse, E., Capalbo, C., Zazzeroni, F., 2017. Cancer secretome and inflammation: The bright and the dark sides of NF-kappaB. Semin Cell Dev Biol.

Chung, J.H., Seo, J.Y., Choi, H.R., Lee, M.K., Youn, C.S., Rhie, G., Cho, K.H., Kim, K.H., Park, K.C., Eun, H.C., 2001. Modulation of skin collagen metabolism in aged and photoaged human skin in vivo. J Invest Dermatol 117(5), 1218-1224.

Claerhout, S., Verschooten, L., Van Kelst, S., De Vos, R., Proby, C., Agostinis, P., Garmyn, M., 2010. Concomitant inhibition of AKT and autophagy is required for efficient cisplatin-induced apoptosis of metastatic skin carcinoma. Int J Cancer 127(12), 2790-2803.

Coppe, J.P., Desprez, P.Y., Krtolica, A., Campisi, J., 2010. The senescence-associated secretory phenotype: the dark side of tumor suppression. Annu Rev Pathol 5, 99-118.

Debacq-Chainiaux, F., Ben Ameur, R., Bauwens, E., Dumortier, E., Toutfaire, M., Toussaint, O., 2016. Stress-Induced (Premature) Senescence, in: Rattan, S.I.S., Hayflick, L. (Eds.), Cellular Ageing and Replicative Senescence. Springer International Publishing, pp. 243-262.

Debacq-Chainiaux, F., Borlon, C., Pascal, T., Royer, V., Eliaers, F., Ninane, N., Carrard, G., Friguet, B., de Longueville, F., Boffe, S., Remacle, J., Toussaint, O., 2005. Repeated exposure of human skin fibroblasts to UVB at subcytotoxic level triggers premature senescence through the TGF-beta1 signaling pathway. J Cell Sci 118(Pt 4), 743-758.

Debacq-Chainiaux, F., Pascal, T., Boilan, E., Bastin, C., Bauwens, E., Toussaint, O., 2008. Screening of senescence-associated genes with specific DNA array reveals the role of IGFBP-3 in premature senescence of human diploid fibroblasts. Free Radic Biol Med 44(10), 1817-1832.

Dierick, J.F., Eliaers, F., Remacle, J., Raes, M., Fey, S.J., Larsen, P.M., Toussaint, O., 2002a. Stress-induced premature senescence and replicative senescence are different phenotypes, proteomic evidence. Biochem Pharmacol 64(5-6), 1011-1017.

Dierick, J.F., Kalume, D.E., Wenders, F., Salmon, M., Dieu, M., Raes, M., Roepstorff, P., Toussaint, O., 2002b. Identification of 30 protein species involved in replicative senescence and stress-induced premature senescence. FEBS Lett 531(3), 499-504.

Dimri, G.P., Lee, X., Basile, G., Acosta, M., Scott, G., Roskelley, C., Medrano, E.E., Linskens, M., Rubelj, I., Pereira-Smith, O., et al., 1995. A biomarker that identifies senescent human cells in culture and in aging skin in vivo. Proceedings of the National Academy of Sciences of the United States of America 92(20), 9363-9367.

Dinarello, C.A., 1996. Biologic basis for interleukin-1 in disease. Blood 87(6), 2095-2147.

Erez, N., Truitt, M., Olson, P., Arron, S.T., Hanahan, D., 2010. Cancer-Associated Fibroblasts Are Activated in Incipient Neoplasia to Orchestrate Tumor-Promoting Inflammation in an NF-kappaB-Dependent Manner. Cancer Cell 17(2), 135-147.

Farsam, V., Basu, A., Gatzka, M., Treiber, N., Schneider, L.A., Mulaw, M.A., Lucas, T., Kochanek, S., Dummer, R., Levesque, M.P., Wlaschek, M., Scharffetter-Kochanek, K., 2016. Senescent fibroblast-derived Chemerin promotes squamous cell carcinoma migration. Oncotarget 7(50), 83554-83569.

Freund, A., Orjalo, A.V., Desprez, P.Y., Campisi, J., 2010. Inflammatory networks during cellular senescence: causes and consequences. Trends Mol Med 16(5), 238-246.

He, S., Sharpless, N.E., 2017. Senescence in Health and Disease. Cell 169(6), 1000-1011.

Kalluri, R., 2016. The biology and function of fibroblasts in cancer. Nat Rev Cancer 16(9), 582-598.

Kalluri, R., Zeisberg, M., 2006. Fibroblasts in cancer. Nat Rev Cancer 6(5), 392-401.

Kaur, A., Webster, M.R., Marchbank, K., Behera, R., Ndoye, A., Kugel, C.H., 3rd, Dang, V.M., Appleton, J., O'Connell, M.P., Cheng, P., Valiga, A.A., Morissette, R., McDonnell, N.B., Ferrucci, L., Kossenkov, A.V., Meeth, K., Tang, H.Y., Yin, X., Wood, W.H., 3rd, Lehrmann, E., Becker, K.G., Flaherty, K.T., Frederick, D.T., Wargo, J.A., Cooper, Z.A., Tetzlaff, M.T., Hudgens, C., Aird, K.M., Zhang, R., Xu, X., Liu, Q., Bartlett, E., Karakousis, G., Eroglu, Z., Lo, R.S., Chan, M., Menzies, A.M., Long, G.V., Johnson, D.B., Sosman, J., Schilling, B., Schadendorf, D., Speicher, D.W., Bosenberg, M., Ribas, A., Weeraratna, A.T., 2016. sFRP2 in the aged microenvironment drives melanoma metastasis and therapy resistance. Nature 532(7598), 250-254.

Kim, E., Rebecca, V., Fedorenko, I.V., Messina, J.L., Mathew, R., Maria-Engler, S.S., Basanta, D., Smalley, K.S., Anderson, A.R., 2013. Senescent fibroblasts in melanoma initiation and progression: an integrated theoretical, experimental, and clinical approach. Cancer Res 73(23), 6874-6885.

Krtolica, A., Parrinello, S., Lockett, S., Desprez, P.Y., Campisi, J., 2001. Senescent fibroblasts promote epithelial cell growth and tumorigenesis: a link between cancer and aging. Proc Natl Acad Sci U S A 98(21), 12072-12077.

Krutmann, J., Bouloc, A., Sore, G., Bernard, B.A., Passeron, T., 2017. The skin aging exposome. J Dermatol Sci 85(3), 152-161.

Lasry, A., Ben-Neriah, Y., 2015. Senescence-associated inflammatory responses: aging and cancer perspectives. Trends Immunol 36(4), 217-228.

Leiter, U., Eigentler, T., Garbe, C., 2014. Epidemiology of skin cancer. Adv Exp Med Biol 810, 120-140.

Li, L., Dragulev, B., Zigrino, P., Mauch, C., Fox, J.W., 2009. The invasive potential of human melanoma cell lines correlates with their ability to alter fibroblast gene expression in vitro and the stromal microenvironment in vivo. Int J Cancer 125(8), 1796-1804.

Lomas, A., Leonardi-Bee, J., Bath-Hextall, F., 2012. A systematic review of worldwide incidence of nonmelanoma skin cancer. Br J Dermatol 166(5), 1069-1080.

Malaquin, N., Martinez, A., Rodier, F., 2016. Keeping the senescence secretome under control: Molecular reins on the senescence-associated secretory phenotype. Exp Gerontol 82, 39-49.

Malaquin, N., Vercamer, C., Bouali, F., Martien, S., Deruy, E., Wernert, N., Chwastyniak, M., Pinet, F., Abbadie, C., Pourtier, A., 2013. Senescent fibroblasts enhance early skin carcinogenic events via a paracrine MMP-PAR-1 axis. PLoS One 8(5), e63607.

Mishra, P., Banerjee, D., Ben-Baruch, A., 2011. Chemokines at the crossroads of tumor-fibroblast interactions that promote malignancy. J Leukoc Biol 89(1), 31-39.

Naylor, R.M., Baker, D.J., van Deursen, J.M., 2013. Senescent cells: a novel therapeutic target for aging and age-related diseases. Clin Pharmacol Ther 93(1), 105-116.

Proby, C.M., Purdie, K.J., Sexton, C.J., Purkis, P., Navsaria, H.A., Stables, J.N., Leigh, I.M., 2000. Spontaneous keratinocyte cell lines representing early and advanced stages of malignant transformation of the epidermis. Exp Dermatol 9(2), 104-117.

Ressler, S., Bartkova, J., Niederegger, H., Bartek, J., Scharffetter-Kochanek, K., Jansen-Durr, P., Wlaschek, M., 2006. p16INK4A is a robust in vivo biomarker of cellular aging in human skin. Aging Cell 5(5), 379-389.

Ruhland, M.K., Loza, A.J., Capietto, A.H., Luo, X., Knolhoff, B.L., Flanagan, K.C., Belt, B.A., Alspach, E., Leahy, K., Luo, J., Schaffer, A., Edwards, J.R., Longmore, G., Faccio, R., DeNardo, D.G., Stewart, S.A., 2016. Stromal senescence establishes an immunosuppressive microenvironment that drives tumorigenesis. Nat Commun 7, 11762.

Toussaint, O., Remacle, J., Dierick, J.F., Pascal, T., Frippiat, C., Royer, V., Magalhacs, J.P., Zdanov, S., Chainiaux, F., 2002. Stress-induced premature senescence: from biomarkers to likeliness of in vivo occurrence. Biogerontology 3(1-2), 13-17.

Toutfaire, M., Bauwens, E., Debacq-Chainiaux, F., 2017. The impact of cellular senescence in skin ageing: A notion of mosaic and therapeutic strategies. Biochem Pharmacol 142, 1-12.

Waaijer, M.E., Parish, W.E., Strongitharm, B.H., van Heemst, D., Slagboom, P.E., de Craen, A.J., Sedivy, J.M., Westendorp, R.G., Gunn, D.A., Maier, A.B., 2012. The number of p16INK4a positive cells in human skin reflects biological age. Aging Cell 11(4), 722-725.

Waldera Lupa, D.M., Kalfalah, F., Safferling, K., Boukamp, P., Poschmann, G., Volpi, E., Gotz-Rosch, C., Bernerd, F., Haag, L., Huebenthal, U., Fritsche, E., Boege, F., Grabe, N., Tigges, J., Stuhler, K., Krutmann, J., 2015. Characterization of Skin Aging-Associated Secreted Proteins (SAASP) Produced by Dermal Fibroblasts Isolated from Intrinsically Aged Human Skin. J Invest Dermatol 135(8), 1954-1968.

Wall, I.B., Moseley, R., Baird, D.M., Kipling, D., Giles, P., Laffafian, I., Price, P.E., Thomas, D.W., Stephens, P., 2008. Fibroblast dysfunction is a key factor in the non-healing of chronic venous leg ulcers. J Invest Dermatol 128(10), 2526-2540.

Zhang, J., Chen, L., Xiao, M., Wang, C., Qin, Z., 2011. FSP1+ fibroblasts promote skin carcinogenesis by maintaining MCP-1-mediated macrophage infiltration and chronic inflammation. Am J Pathol 178(1), 382-390.

Captions of figures

Fig. 1. *Impact of senescent dermal HDFs-conditioned media on cutaneous squamous cell carcinoma (cSCC) cell lines growth.*

Conditioned media were collected after 48 hours of incubation with media alone (BME) or from young (Y), replicative senescent (RS), control of stress-induced premature senescent (CTL-SIPS) or SIPS human diploid fibroblasts (HDFs). (A) PM1, (B) MET1 and (C) MET4 cell growths were measured after 24 hours of incubation with conditioned media using MTS assay. It is represented as the mean percentage of cell growth when compared with BME ± SEM from three independent experiments with technical triplicates (**p<0.01, ***p<0.001).

Fig. 2. *Impact of senescent dermal HDFs-conditioned media on cutaneous squamous cell carcinoma (cSCC) cell lines migration.*

Conditioned media were collected after 48 hours of incubation with media alone (BME) or from young (Y), replicative senescent (RS), control of stress-induced premature senescent (CTL-SIPS) or SIPS human diploid fibroblasts (HDFs). (A) PM1, (B) MET1 and (C) MET4 migrating cells were counted after 24 hours of incubation with conditioned media as attractant using Boyden Chambers. It is represented as the mean percentage when compared with BME ± SEM from three independent experiments with technical triplicates (*p<0.05, **p<0.01, ***p<0.001).

Fig. 3. *Impact of senescent dermal HDFs-conditioned media on cutaneous squamous cell carcinoma (cSCC) cell lines invasion.*

Conditioned media were collected after 48 hours of incubation with media alone (BME) or from young (Y), replicative senescent (RS), control of stress-induced premature senescent (CTL-SIPS) or SIPS human diploid fibroblasts (HDFs). (A)

MET1 and (B) MET4 invading cells were counted after 24 hours of incubation with conditioned media as attractant using matrigel coated-Boyden Chambers. It is represented as the mean percentage when compared with BME ± SEM from three independent experiments with technical triplicates (**p<0.01, ***p<0.001).

Fig. 4. *Experimental design and time frame of the indirect co-cultures.*

Young dermal human diploid fibroblasts (HDFs) were cultivated during several months until replicative senescence. UVB-stress-induced premature senescence (UVB-SIPS) HDFs were obtained according to the protocol described in (Debacq-Chainiaux et al., 2005). Briefly, young HDFs were exposed to UVB (250 mJ/cm^2) twice a day during five days and then collected after 72h of recovery. For indirect co-culture experiments, HDFs were seeded into wells at day -1. Cutaneous squamous cell carcinoma (cSCC) cell lines were seeded into transwells at day 0. Co-cultures analyses were then performed at day 1, 3 and 6. Culture media were changed on day 3.

Fig. 5. *Impact of senescent dermal HDFs-co-cultures on cutaneous squamous cell carcinoma (cSCC) cell lines growth.*

(A) PM1, (B) MET1 and (C) MET4 relative growths were measured after 1, 3 and 6 days of co-culture using MTS assay. Co-cultures were performed with young (+ Y), replicative senescent (+ RS), control of stress-induced premature senescent (+ CTL) or SIPS human diploid fibroblasts (HDFs) using transwell. Results show the relative growth ratio (when compared with Y or CTL at day 1) ± SEM from four independent experiments for RS HDFs-co-cultures and three independent experiments for SIPS HDFs-co-cultures (*p<0.05, **p<0.01).

Fig. 6. *Impact of cutaneous squamous cell carcinoma (cSCC) cell lines-co-cultures on percentage of senescence-associated-β galactosidase (SA-βgal) positive dermal HDFs.*

Young (Y) or replicative senescent (RS) human diploid fibroblasts (HDFs) were maintained in co-culture alone or with PM1, MET1 or MET4 using transwell. At day 1 and 6 of co-culture, HDFs were reseeded and stained for SA-βgal activity the next day. Results are represented as the mean percentage of SA-βgal positive HDFs ± SEM (400 cells were counted per condition) from one experiment with technical triplicates ($^{\#}$ comparison between alone and +PM1/+MET1/+MET4, $^{*,\#}p<0.05$, $^{**}p<0.01$,$^{\#\#}$,$^{***}p<0.001$).

Fig. 7. *Impact of cutaneous squamous cell carcinoma (cSCC) cell lines-co-cultures on senescence-associated secretory phenotype (SASP) mRNA abundances in young and replicative senescent dermal HDFs.*

(A) *CCL2*, (B) *IL1B* and (C) *IL8* relative mRNA abundances. Young (Y) or replicative senescent (RS) human diploid fibroblasts (HDFs) were maintained in co-culture alone or with PM1, MET1 or MET4 using transwell. At day 1 and 6 of co-culture, relative mRNA abundances were measured by RT-qPCR. Fold changes are normalized to the mRNA abundance of glyceraldehyde-3-phosphate dehydrogenase (*GAPDH*), and are expressed relative to Y alone at day 1. Results are represented as the mean log2 fold change ± SEM from four independent experiments ($^{\#}$ comparison between alone and +PM1/+MET1/+MET4, $^{*,\#,\$}p<0.05$, $^{\#\#}p<0.01$, $^{***,\#\#\#}p<0.001$).

Fig. 8. *Impact of A431-co-culture on SASP mRNA abundances in young and replicative senescent dermal HDFs.* (A) *CCL2*, (B) *IL1B* and (C) *IL8* relative mRNA abundances.

Young (Y) or replicative senescent (RS) human diploid fibroblasts (HDFs) were maintained in co-culture alone or with A431 using transwell. At day 1 and 3 of co-culture, relative mRNA abundances were measured by RT-qPCR. Fold changes are normalized to the mRNA abundance of glyceraldehyde-3-phosphate dehydrogenase (*GAPDH*), and are expressed relative to Y alone at day 1. Results are represented as the mean log2 fold change ± SEM from two independent experiments in technical duplicates ($^{*,\#}p<0.05$, $^{**}p<0.01$, $^{***}p<0.001$).

Fig. 9. *Impact of cutaneous squamous cell carcinoma (cSCC) cell lines-co-cultures on nuclear p65 intensity in young and replicative senescent dermal HDFs.*

(A) Representative immunofluorescence staining images and quantification of nuclear p65 intensity in negative and positive controls (fibroblasts incubated without or with tumor necrosis factor-alpha) are shown. Montage images (of 3 x 3 containing 9 adjacent image fields) were acquired using a 20X objective. (B) Immunofluorescence staining quantification in PM1-, MET1- and MET4-co-cultures. (C) Immunofluorescence staining quantification in A431-co-cultures. Young (Y) and replicative senescent (RS) human diploid fibroblasts (HDFs) were maintained in co-culture alone or with PM1, MET1, MET4 (for 6 days) or A431 (for 3 days) using transwell. p65 fluorescence intensity was measured in the nucleus using BD Pathway 855. Results are represented as the mean fluorescence intensity per cell ± SEM (an average of 250 cells was counted per condition) from one experiment ($^{\#}$ comparison between alone and +PM1/+MET1/+MET4/+A431, $^{\$\$}p<0.01$, $^{***,\#\#\#,\$\$\$}p<0.001$).

Fig. 10. *Impact of cutaneous squamous cell carcinoma (cSCC) cell lines-co-cultures on IκBα protein abundance in young and replicative senescent dermal HDFs.*

Representative western blot analysis of IκBα (nuclear factor-kappa B inhibitor alpha) in (A) negative and positive controls (fibroblasts incubated without or with tumor necrosis factor-alpha) and (B) young (Y) or replicative senescent (RS) human diploid fibroblasts (HDFs) maintained in co-culture alone or with PM1, MET1, MET4 for 6 days using transwell. β-actin was used as loading control. Results originate from the same immunoblot at the indicated molecular weight (MW). (C-D) Quantification of the relative abundance of IκBα. Signal intensities were quantified, normalized to the abundance of β-actin, and are expressed relative to CTL - (C) or Y alone (D). Results are represented as the mean fold change ± SEM from technical duplicates (C) or triplicates (D) ($^{\#}$ comparison between alone and +PM1/+MET1/+MET4, *p<0.05, $^{\#}$ $^{\#}$p<0.01, $^{\#\#\#}$p<0.001).

Fig. 11. *Possible signaling between cutaneous squamous cell carcinoma (cSCC) cell lines and dermal HDFs.*

Co-cultures between cSCC cell lines and dermal human diploid fibroblasts (HDFs) allow bidirectional exchanges. Extracellular signaling from cSCC cell lines induces senescence and senescence-associated secretory phenotype (SASP) expression in young HDFs and reinforces SASP in replicative senescent HDFs. This might involve an activation of nuclear factor-kappa B (NF-κB) and/or other transcription factors such as C/EBPβ (CCAAT/enhancer binding protein beta) in HDFs. It results in cSCC cell lines growth, and may impact migration and invasion. Overall these exchanges are modulated by the SCC cell lines' tumorigenesis stage.

Tables

Table 1. *Screening of the senescence-associated secretory phenotype (SASP)-related mRNA abundances in senescent dermal HDFs***.**

Gene	Name	Fold change	p-value	
(A)		RS		
IL1B	Interleukin 1 beta	9.08	0.011	*
ICAM1	Intercellular adhesion molecule 1	2.65	0.012	*
CTGF	Connective tissue growth factor	2.56	0.001	**
IL6	Interleukin 6	2.52	0.002	**
CXCL2	C-X-C motif chemokine ligand 2	0.46	0.027	*
IGFBP2	Insulin like growth factor binding protein 2	0.40	0.052	*
CXCL1	C-X-C motif chemokine ligand 1	0.37	0.001	**
HGF	Hepatocyte growth factor	0.31	0.010	*
MMP3	Matrix metallopeptidase 3	0.27	0.005	**
(B)		SIPS		
MMP3	Matrix metallopeptidase 3	8.46	0.003	**
CXCL1	C-X-C motif chemokine ligand 1	4.82	0.000	***
IL1B	Interleukin 1 beta	3.05	0.030	*
CTGF	Connective tissue growth factor	2.95	0.002	**
IL8	Interleukin 8	2.71	0.048	*
CCL2	C-C motif chemokine ligand 2	2.58	0.013	*
FGF2	Fibroblast growth factor 2	2.57	0.002	**
MMP1	Matrix metallopeptidase 1	2.41	0.022	*
IL6	Interleukin 6	2.37	0.047	*
IGFBP6	Insulin like growth factor binding protein 6	2.05	0.024	*
IGFBP3	Insulin like growth factor binding protein 3	1.81	0.009	**
CXCL2	C-X-C motif chemokine ligand 2	1.69	0.005	**
TIMP2	TIMP metallopeptidase inhibitor 2	1.61	0.001	**
TGFB1	Transforming growth factor beta 1	1.61	0.049	*

(A) Relative mRNA abundances in replicative senescent (RS) HDFs. (B) Relative mRNA abundances in UVB stress-induced premature senescent (SIPS) HDFs. Relative mRNA abundances were measured using TaqMan Low Density Arrays (TLDA) from five independent experiments for RS and from four independent experiments for SIPS. Fold changes are normalized to the mRNA abundance of glyceraldehyde-3-phosphate dehydrogenase (*GAPDH*), and are expressed relative to young or CTL-SIPS HDFs. The significant changes are represented (*$p<0.05$, **$p<0.01$, ***$p<0.001$).

Table 2. *Screening of senescence-associated secretory phenotype (SASP)-related mRNA abundances in young and replicative senescent dermal HDFs after 6 days of co-culture with cutaneous squamous cell carcinoma (cSCC) cell lines.*

Gene	Name	Fold change (relative to Y alone at day 1)						Impact of senescence		Impact of co-culture		*Post hoc* test for co-culture
		Y alone	Y + PM1	Y + MET1	RS alone	RS + PM1	RS + MET1					
CCL2	C-C motif chemokine ligand 2	4.7	22.1	42.8	15.5	63.5	82.7	↑	*	↑	*	+ PM1 ($^{\#}$), + MET1 ($^{\#}$)
CXCL2	C-X-C motif chemokine ligand 2	2.6	32.1	38.6	4.2	60.5	69.7	↑	**	↑	***	+ PM1 ($^{\#\#\#}$), + MET1 ($^{\#\#\#}$)
IL1B	Interleukin 1 beta	0.4	4.7	5.7	3.4	19.7	25.5	↑	*	↑	*	+ PM1 ($^{\#}$), + MET1 ($^{\#}$)
MMP1	Matrix metallopeptidase 1	0.0	0.1	0.1	0.2	0.4	0.5	↑	**	↑	*	+ PM1 ($^{\#}$), + MET1 ($^{\#}$)
TIMP2	TIMP metallopeptidase inhibitor 2	1.5	1.3	1.3	1.8	1.6	1.7	↑	**	↓	*	+ PM1 ($^{\#}$)
CCL20	C-C motif chemokine ligand 20	7.5	67.7	122.8	11.9	347.2	349.5	NS		↑	*	+ PM1 ($^{\#}$), + MET1 ($^{\#}$)
CXCL1	C-X-C motif chemokine ligand 1	1.1	45.2	91.6	0.5	50.8	87.7	NS		↑	*	+ PM1 ($^{\#}$), + MET1 ($^{\#}$)
ICAM1	Intercellular adhesion molecule 1	7.6	17.3	22.5	9.7	17.1	19.4	NS		↑	*	+ MET1 ($^{\#}$)
IL8	Interleukin 8	0.9	51.6	92.9	0.8	141.3	175.0	NS		↑	*	+ PM1 ($^{\#}$), + MET1 ($^{\#}$)
FGF2	Fibroblast growth factor 2	0.5	0.7	0.6	1.0	1.0	1.1	↑	*	NS		NS
IGFBP3	Insulin like growth factor binding protein 3	0.9	0.9	0.8	2.5	1.8	2.6	↑	*	NS		NS
IGFBP5	Insulin like growth factor binding protein 5	0.2	0.2	0.2	0.4	0.3	0.3	↑	*	NS		NS
MMP3	Matrix metallopeptidase 3	0.0	0.1	0.1	0.4	1.6	1.3	↑	*	NS		NS
MMP10	Matrix metallopeptidase 10	0.1	0.1	0.1	0.4	0.2	0.3	↑	*	NS		NS
TNFRSF11B	TNF receptor superfamily member 11B	1.1	0.9	1.1	3.7	2.6	2.8	↑	**	NS		NS
IGFBP2	Insulin like growth factor binding protein 2	5.5	5.8	4.7	2.8	1.6	1.8	↓	*	NS		NS
PTGS1	Prostaglandin-endoperoxide synthase 1	0.4	0.7	0.4	0.1	0.1	0.1	↓	**	NS		NS
VCAM1	Vascular cell adhesion molecule 1	19.7	33.0	32.6	5.7	13.0	13.6	↓	*	NS		NS

Young (Y) or replicative senescent (RS) HDFs were maintained in co-culture alone or with PM1 or MET1 using transwell. Relative mRNA abundances were measured using TaqMan Low Density Arrays (TLDA) from one experiment. Fold changes are normalized to the mRNA abundance of glyceraldehyde-3-phosphate dehydrogenase (*GAPDH*) and *RNA18S*, and are expressed relative to Y alone at day 1 of co-culture. The significant impact of senescence and / or co-culture is represented in three categories: impact of

senescence and co-culture; impact of co-culture and impact of senescence (↑ upregulation, ↓ repression, NS non significant). If co-culture impact was significant, Tukey was used as *post hoc* test ($^{\#}$ comparison between alone and + PM1 or + MET1). $^{*,\#}p<0.05$, $^{**}p<0.01$, $^{***,\#\#\#}p<0.001$.

iraphical Abstract

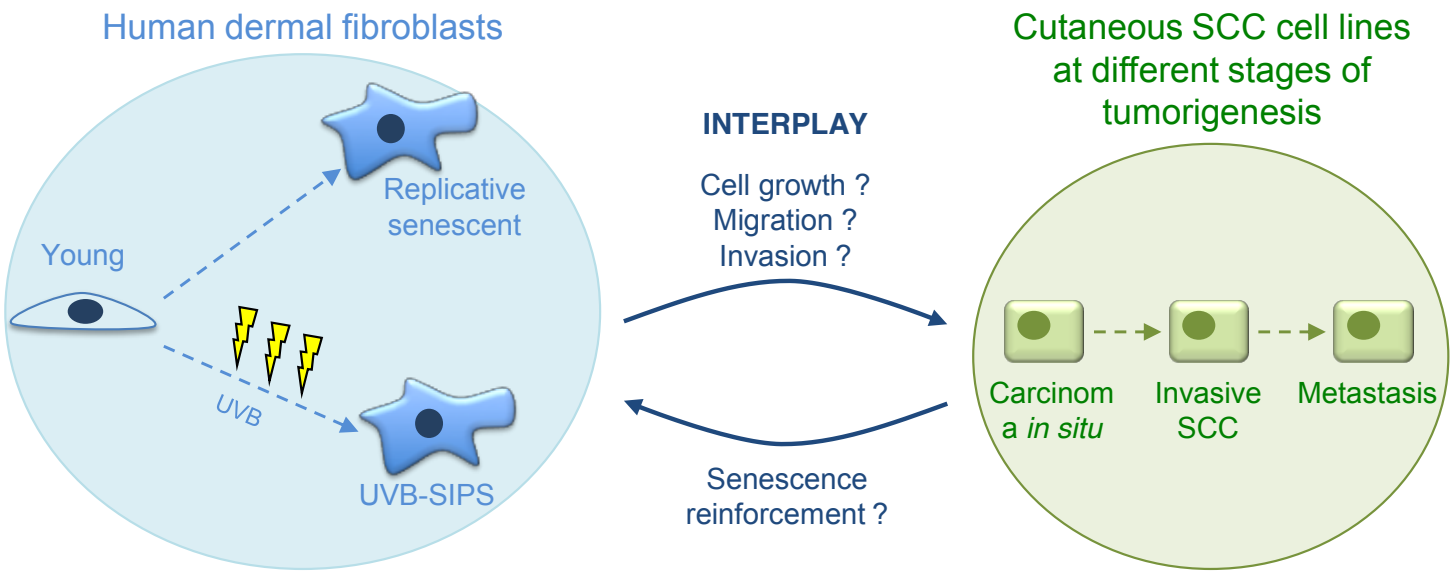

A.

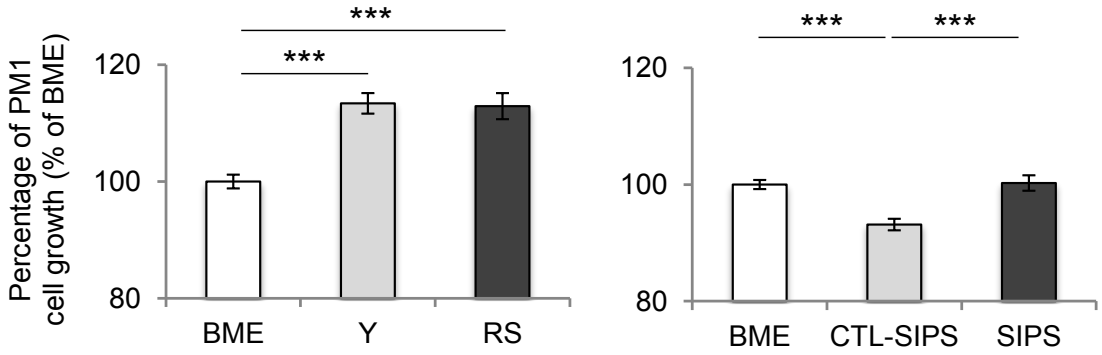
Percentage of PM1 cell growth (% of BME)
120
100
80
***
***
BME
Y
RS
***
***
120
100
80
BME
CTL-SIPS
SIPS

B.

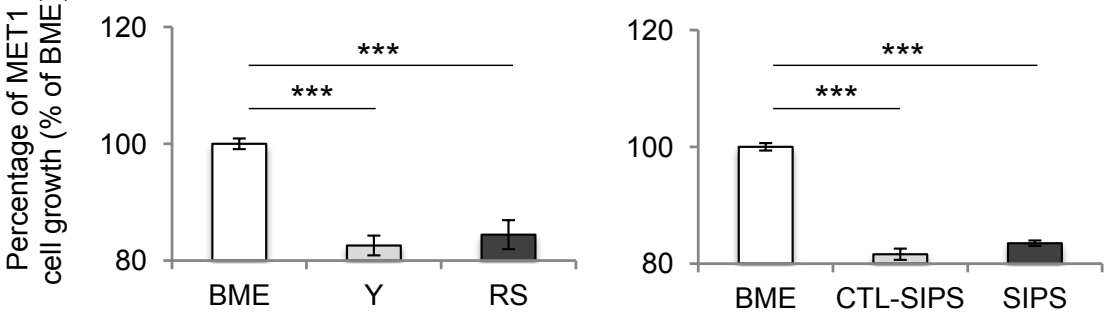
Percentage of MET1 cell growth (% of BME)
120
100
80
***
***
BME
Y
RS
120
100
80
***
***
BME
CTL-SIPS
SIPS

C.

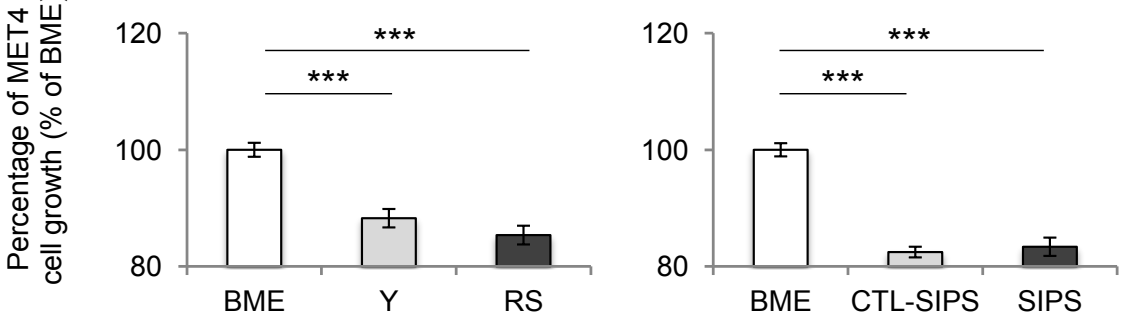
Percentage of MET4 cell growth (% of BME)
120
100
80
***
***
BME
Y
RS
120
100
80
***
***
BME
CTL-SIPS
SIPS

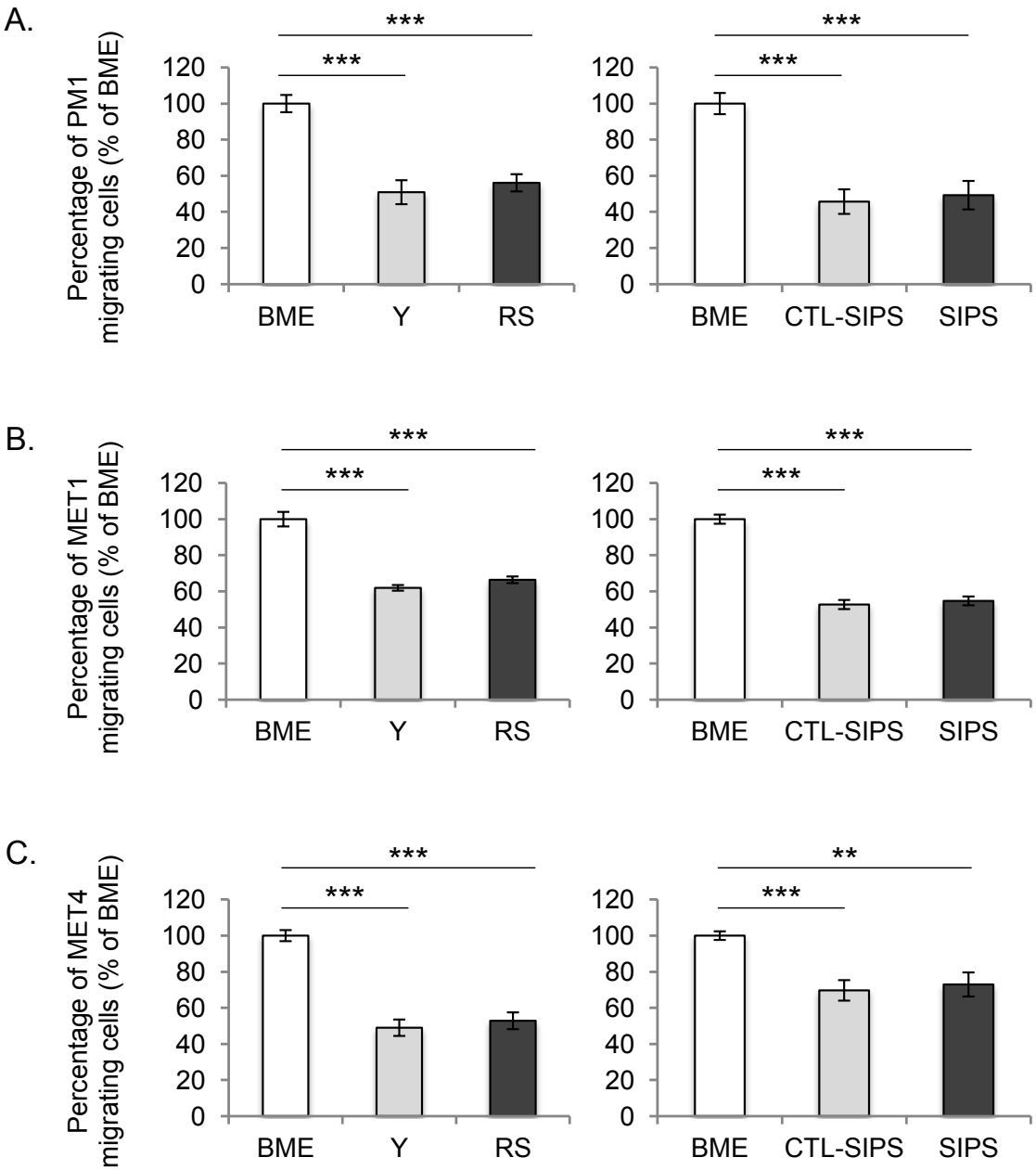
A.
Percentage of PM1 migrating cells (% of BME)
***
***
120
100
80
60
40
20
0
BME
Y
RS
***
***
120
100
80
60
40
20
0
BME
CTL-SIPS
SIPS
B.
Percentage of MET1 migrating cells (% of BME)
***
***
120
100
80
60
40
20
0
BME
Y
RS
***
***
120
100
80
60
40
20
0
BME
CTL-SIPS
SIPS
C.
Percentage of MET4 migrating cells (% of BME)
***
***
120
100
80
60
40
20
0
BME
Y
RS
**
***
120
100
80
60
40
20
0
BME
CTL-SIPS
SIPS

A.

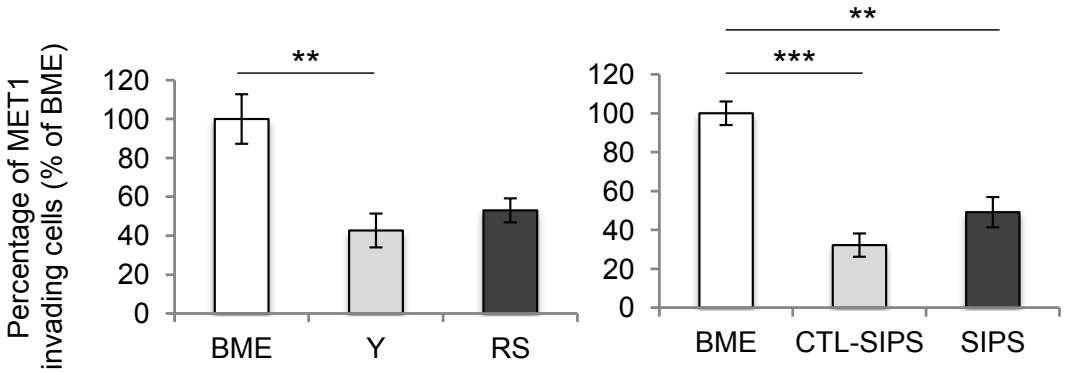
Percentage of MET1 invading cells (% of BME)
120
100
80
60
40
20
0
**
BME
Y
RS
**
***
BME
CTL-SIPS
SIPS

B.

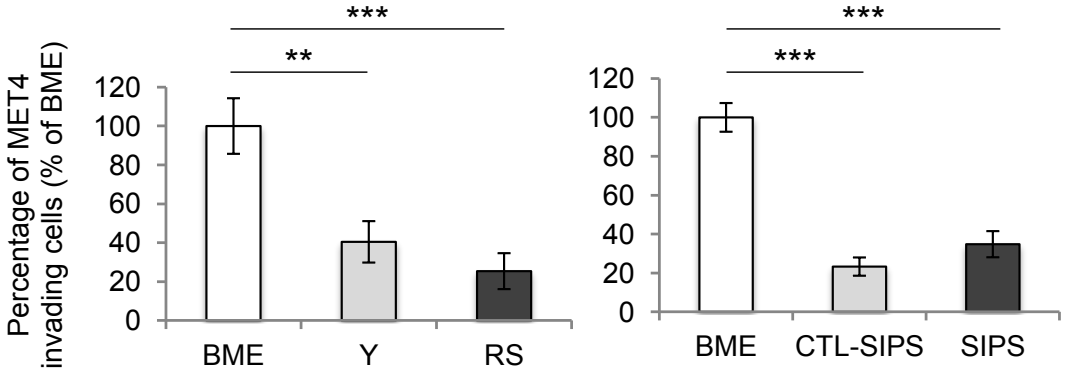
Percentage of MET4 invading cells (% of BME)
120
100
80
60
40
20
0
***
**
BME
Y
RS
***
***
BME
CTL-SIPS
SIPS

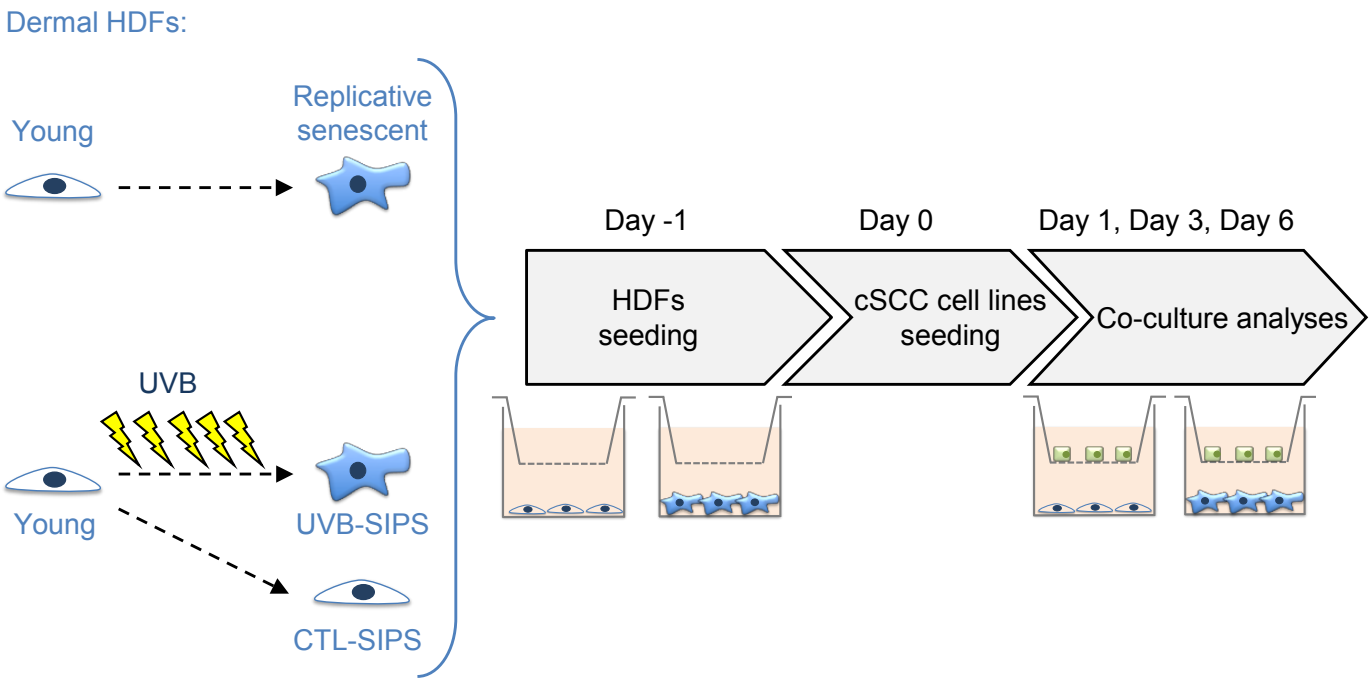
Dermal HDFs:
Young
Replicative senescent
UVB
Young
UVB-SIPS
CTL-SIPS
Day -1
Day 0
Day 1, Day 3, Day 6
HDFs seeding
cSCC cell lines seeding
Co-culture analyses

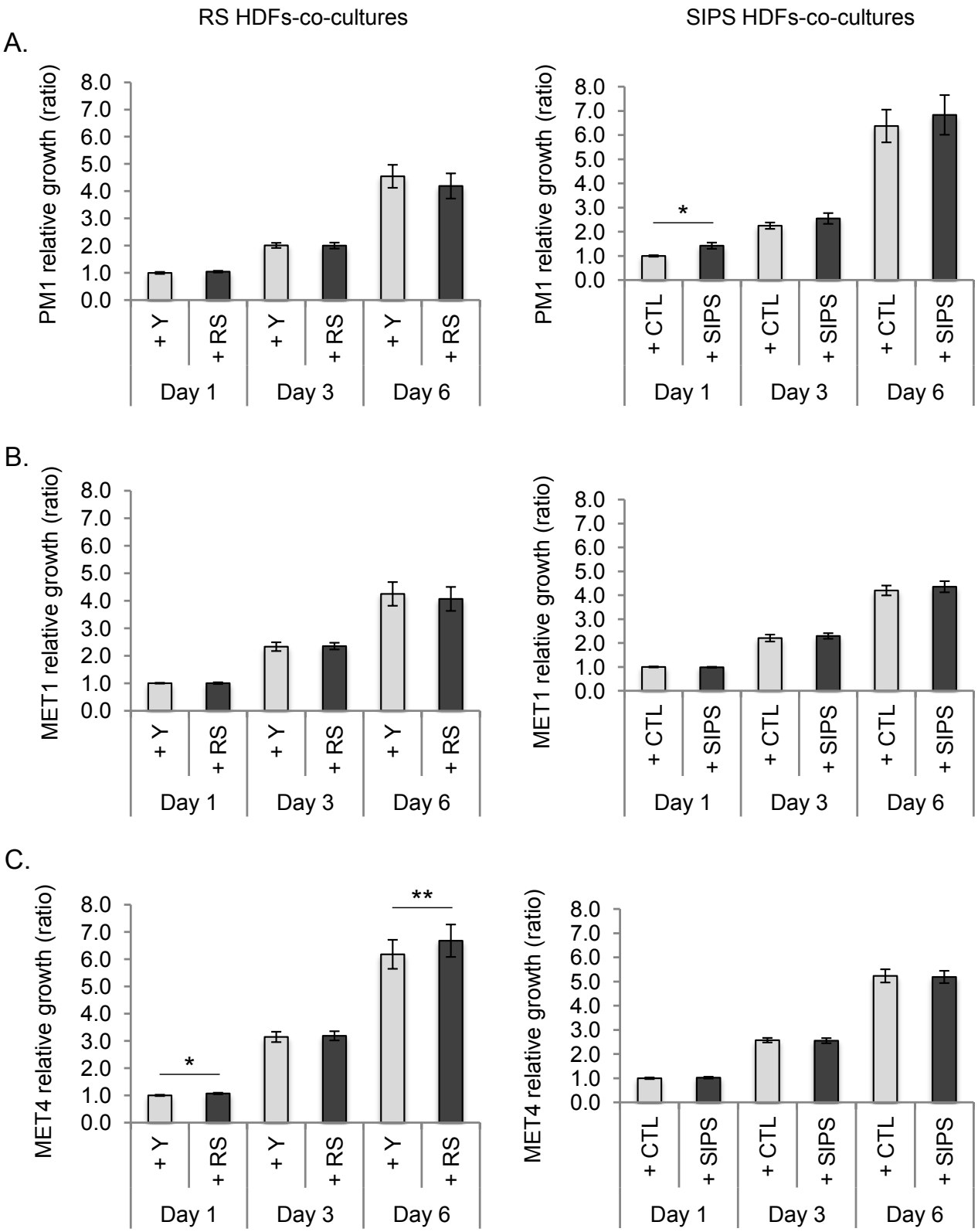
RS HDFs-co-cultures
SIPS HDFs-co-cultures
A.
PM1 relative growth (ratio)
B.
MET1 relative growth (ratio)
C.
MET4 relative growth (ratio)
+ Y
+ RS
+ CTL
+ SIPS
Day 1
Day 3
Day 6
*
**

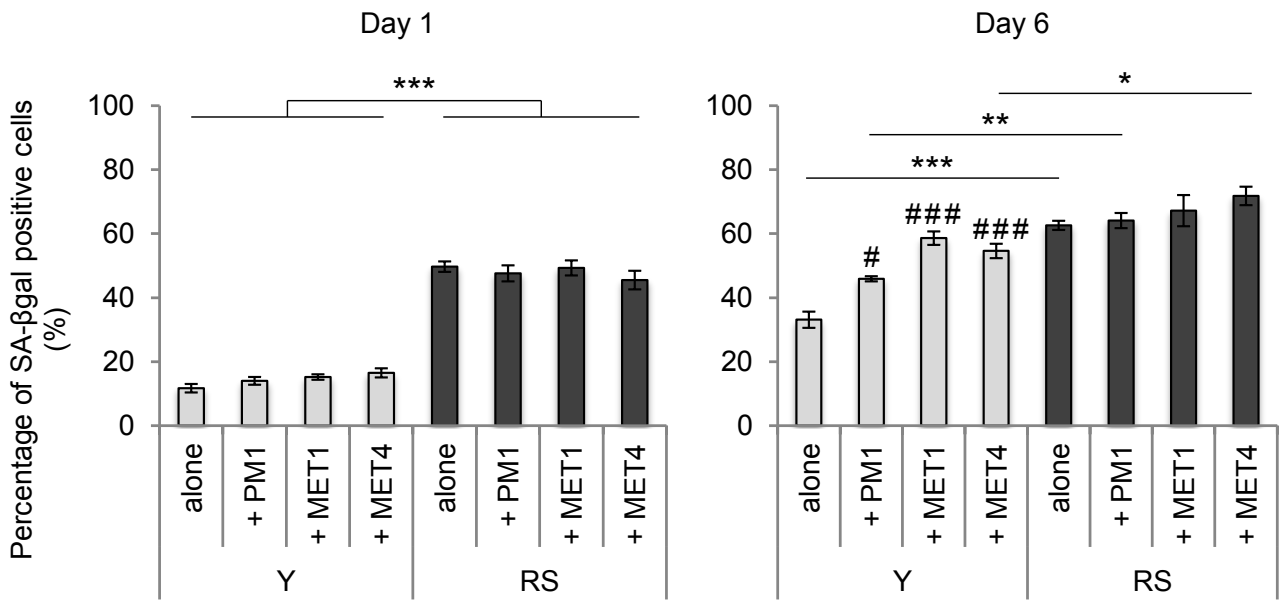
Day 1
Day 6
Percentage of SA-βgal positive cells (%)
100
80
60
40
20
0
***
*
**
***
#
###
###
alone
+ PM1
+ MET1
+ MET4
Y
RS

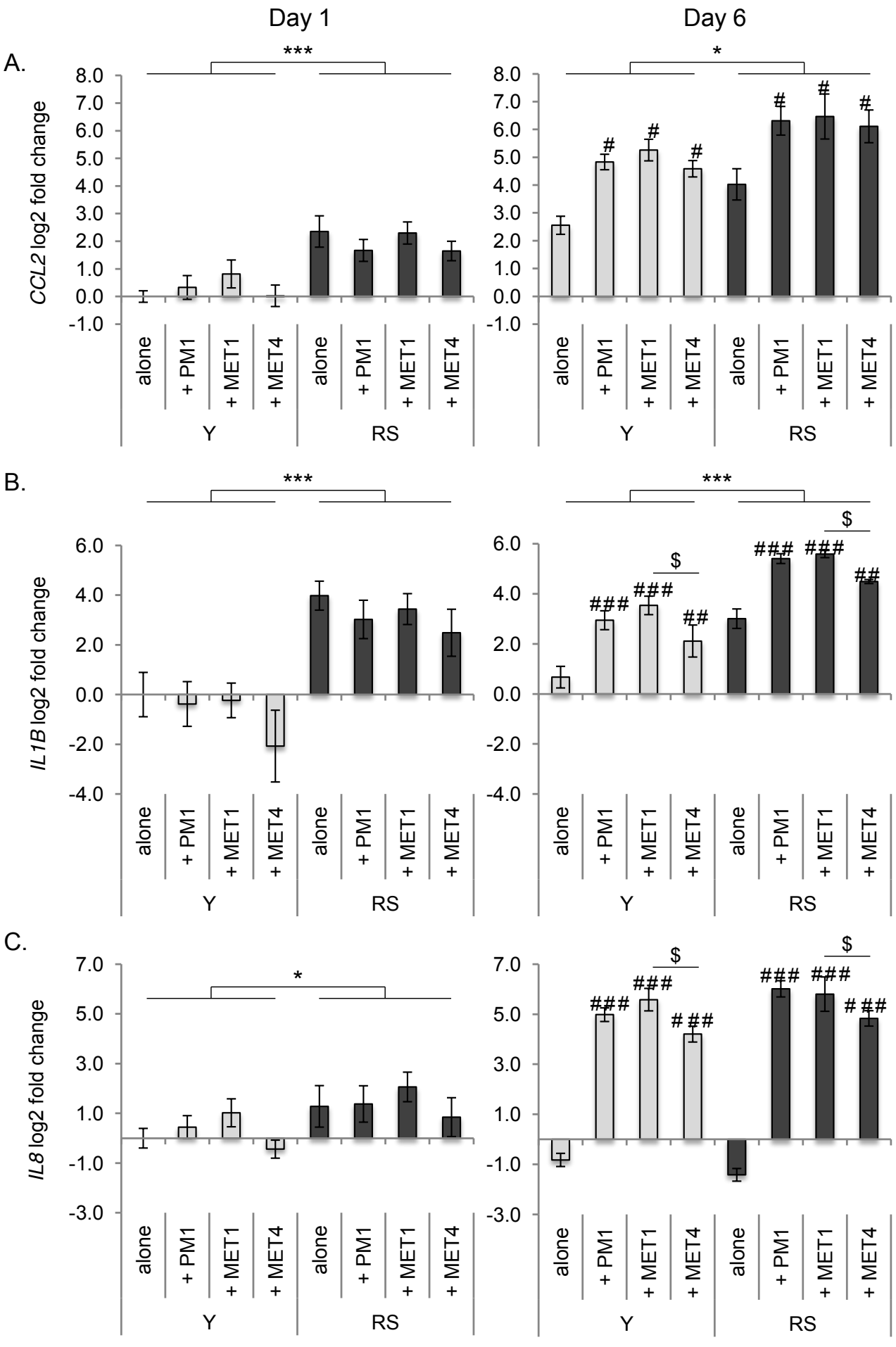
Day 1
Day 6
A.
B.
C.
CCL2 log2 fold change
IL1B log2 fold change
IL8 log2 fold change
alone
+ PM1
+ MET1
+ MET4
Y
RS
***
*
$
#
##
###

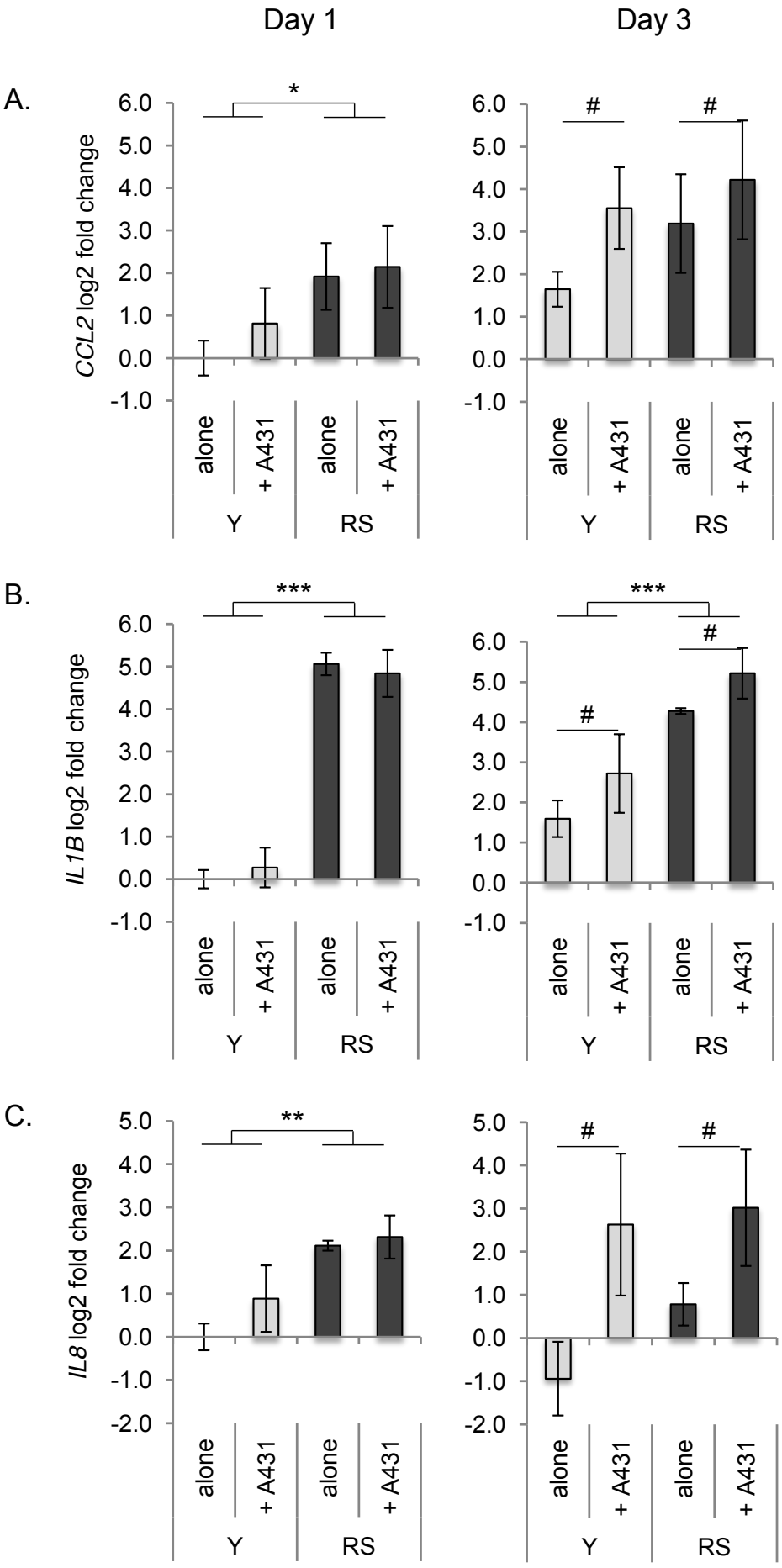
Day 1
Day 3
A.
CCL2 log2 fold change
B.
IL1B log2 fold change
C.
IL8 log2 fold change
alone
+ A431
Y
RS
*
**
***
#

A.

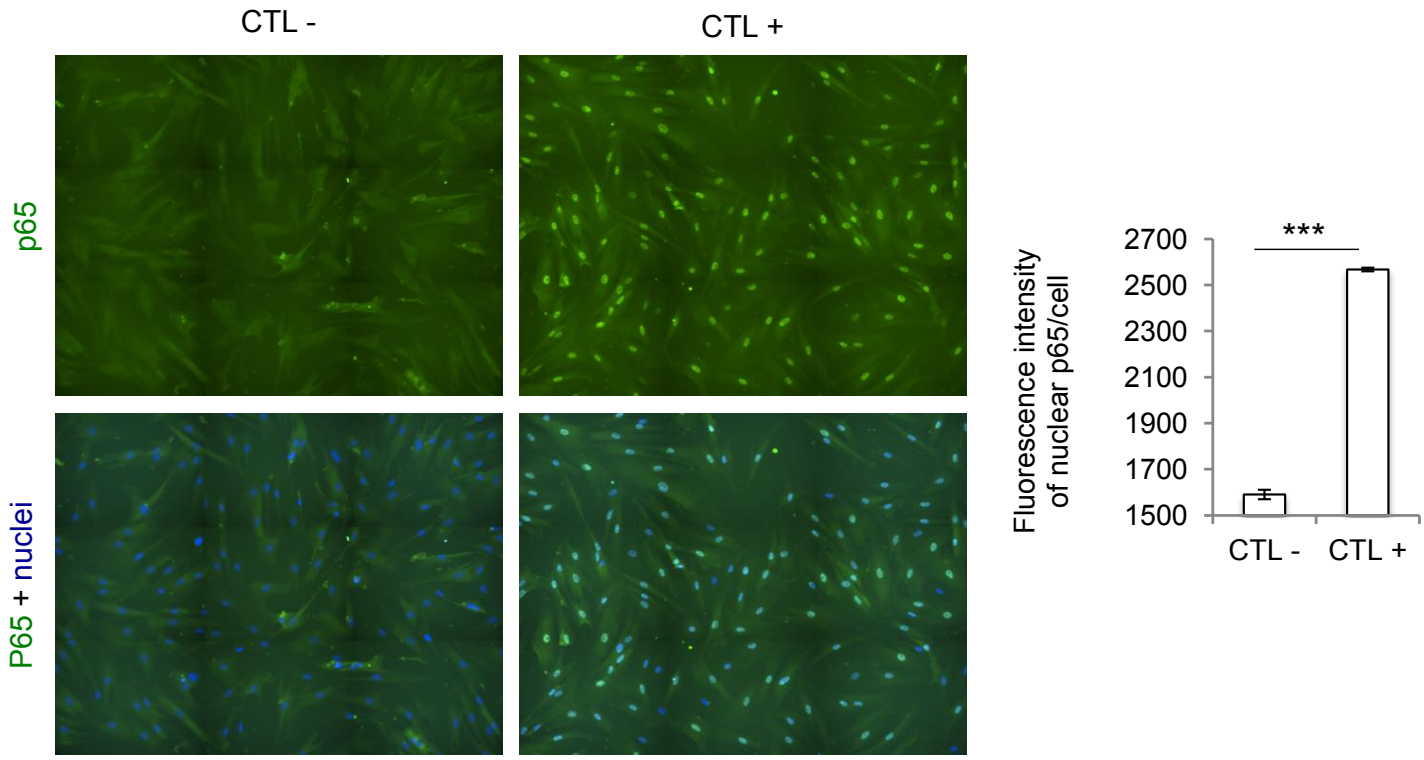
CTL -
CTL +
p65
P65 + nuclei
Fluorescence intensity of nuclear p65/cell
2700
2500
2300
2100
1900
1700
1500
***
CTL -
CTL +

B.

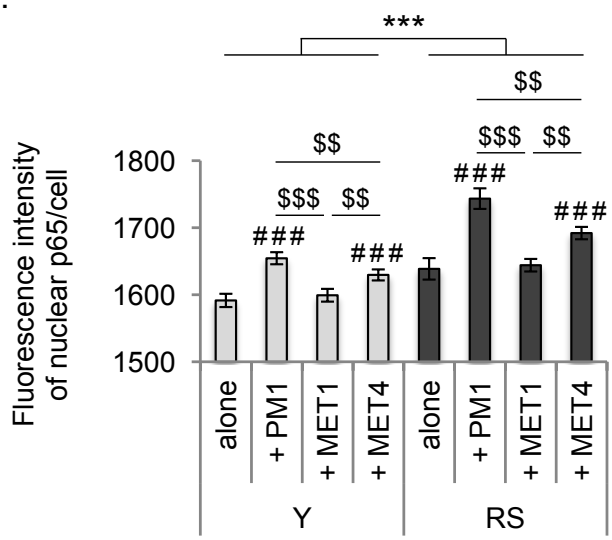
Fluorescence intensity of nuclear p65/cell
1800
1700
1600
1500
***
$$
$$$
$$
$$$
$$
###
###
###
###
alone
+ PM1
+ MET1
+ MET4
alone
+ PM1
+ MET1
+ MET4
Y
RS

C.

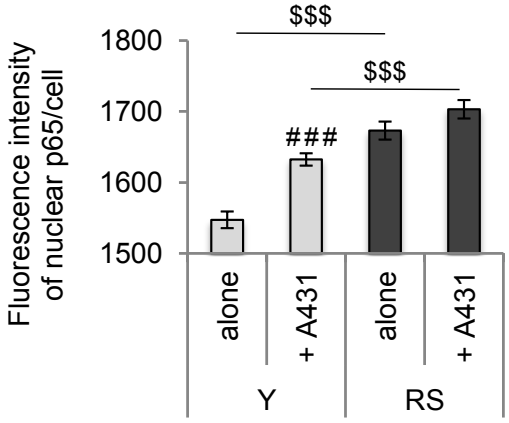
Fluorescence intensity of nuclear p65/cell
1800
1700
1600
1500
$$$
$$$
###
alone
+ A431
alone
+ A431
Y
RS

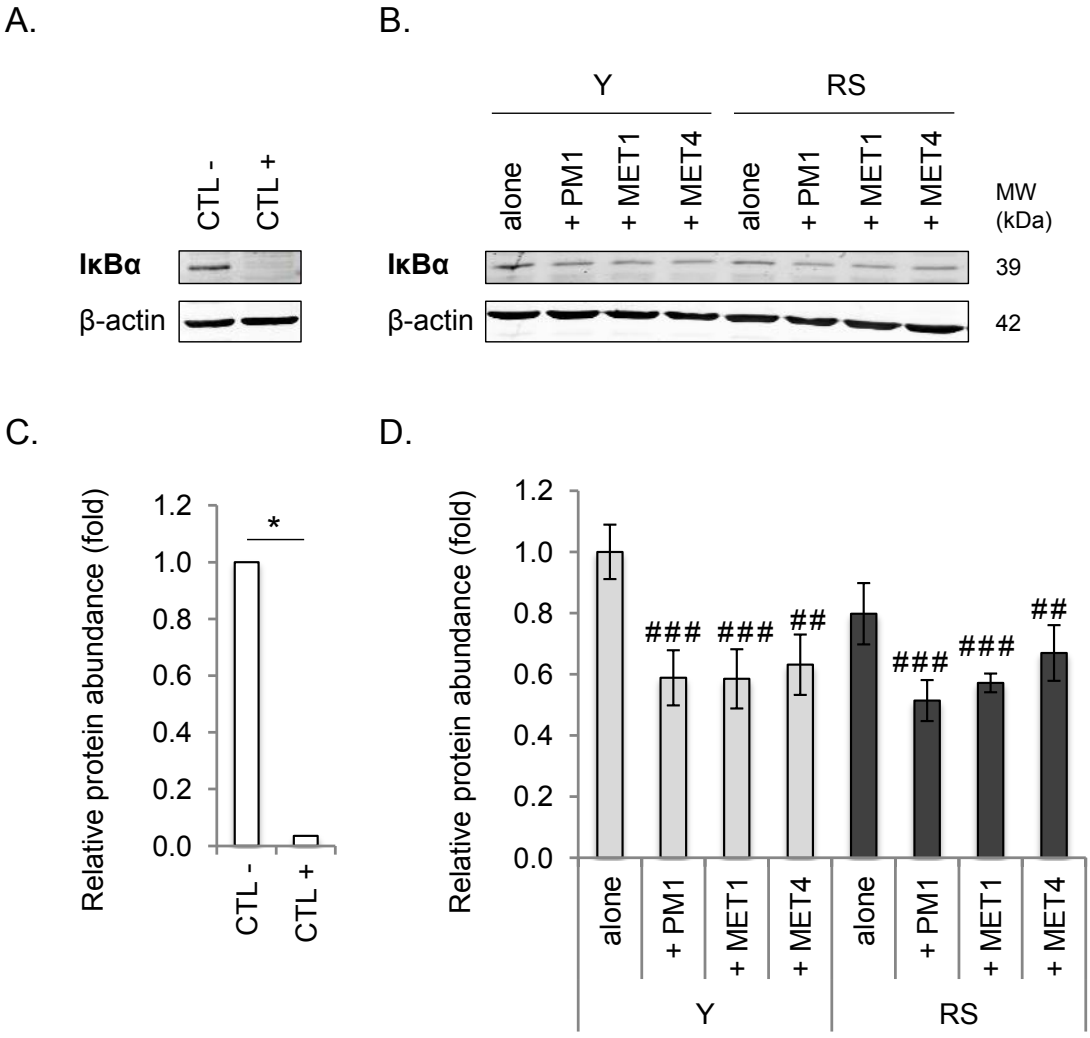
A.
B.
CTL -
CTL +
IκBα
β-actin
Y
RS
alone
+ PM1
+ MET1
+ MET4
MW (kDa)
39
42
C.
D.
Relative protein abundance (fold)
1.2
1.0
0.8
0.6
0.4
0.2
0.0
*
###
##

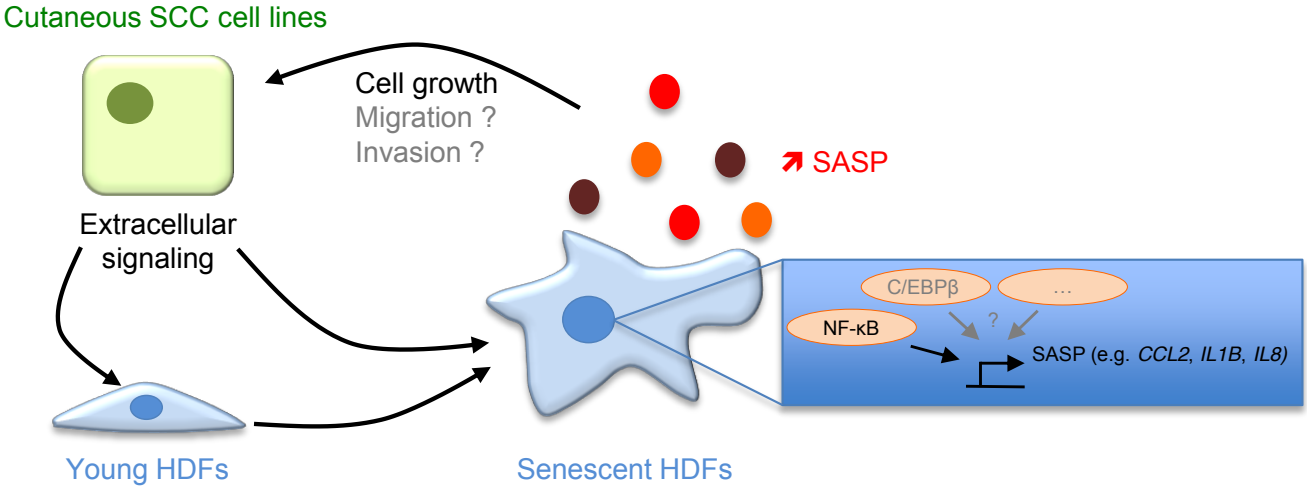
Cutaneous SCC cell lines
Cell growth
Migration ?
Invasion ?
SASP
Extracellular
signaling
C/EBPβ
…
NF-κB
?
SASP (e.g. CCL2, IL1B, IL8)
Young HDFs
Senescent HDFs

upplementary Manuscript
lick here to download Supplementary Files: BC-D-1700454 supplementary data.docx

arked Supplementary Manuscript
lick here to download Supplementary Files: BC-D-1700454 supplementary data_revision notes.docx

upplementary Figure 1
lick here to download Supplementary Files: FIGS1.PPTX

upplementary Figure 2
lick here to download Supplementary Files: FIGS2.PPTX

upplementary Figure 3

lick here to download Supplementary Files: FIGS3.PPTX

upplementary Figure 4
lick here to download Supplementary Files: FIGS4.PPTX

upplementary Figure 5
lick here to download Supplementary Files: FIGS5.PPTX

upplementary Figure 6
lick here to download Supplementary Files: FIGS6.PPTX

upplementary Figure 7
lick here to download Supplementary Files: FIGS7.PPTX

upplementary Figure 8
lick here to download Supplementary Files: FIGS8.PPTX

upplementary Figure 9
lick here to download Supplementary Files: FIGS9.PPTX

upplementary Figure 10
lick here to download Supplementary Files: FIGS10.PPTX

upplementary Figure 11
lick here to download Supplementary Files: FIGS11.PPTX

upplementary Figure 12

lick here to download Supplementary Files: FIGS12.PPTX